REPUBLIC OF TURKIYE

ALTINBAŞ UNIVERSITY

Institute of Graduate Studies

Electrical and Computer Engineering

DESIGN AND ENHANCEMENT OF MICROSTRIP PATCH ANTENNA FOR PERSONAL NETWORKS IN THE GOVERNMENT INSTITUTIONS

Saif AL-ATTAR

Master's Thesis

Supervisor

Asst. Prof. Dr. Abdullahi Abdu IBRAHIM

Istanbul, 2022

DESIGN AND ENHANCEMENT OF MICROSTRIP PATCH ANTENNA FOR PERSONAL NETWORKS IN THE GOVERNMENT INSTITUTIONS

Saif AL-ATTAR

Electrical and Computer Engineering

Master's Thesis

ALTINBAŞ UNIVERSITY

2022

The thesis titled DESIGN AND ENHANCEMENT OF MICROSTRIP PATCH ANTENNA FOR PERSONAL NETWORKS IN THE GOVERNMENT INSTITUTIONS prepared by SAIF MOHAMMED KADHIM KAMAL AL-ATTAR and submitted on 08/0/ 2022 has been **accepted unanimously** for the degree of Master of Science in Electrical and Computer Engineering.

Asst. prof. Dr. Abdullahi Abdu IBRAHIM

Supervisor

Thesis Defense Committee Members:

Asst. Prof. Dr. Abdullahi Abdu IBRAHIM	Faculty of Engineering and Architecture, Altinbas University	_____
Asst. Prof. Dr. Oguz KARAN	Faculty of Engineering and Architecture, Altinbas University	_____
Asst. Prof. Dr. Tareq Abed MOHAMMED	Faculty of Computer Science and Information Technology, Kirkuk University	_____

I hereby declare that this thesis meets all format and submission requirements of a Master's thesis.

Submission date of the thesis to the Institute of Graduate Studies: ____/____/____

I hereby declare that all information/data presented in this graduation project has been obtained in full accordance with academic rules and ethical conduct. I also declare all unoriginal materials and conclusions have been cited in the text and all references mentioned in the Reference List have been cited in the text, and vice versa as required by the abovementioned rules and conduct.

SAIF AL-ATTAR

Signature

DEDICATION

In the name of Allah, the Merciful…

It may not be enough to contain words of thanks to Allah for the strength and hope that makes me believe that this work. It would be possible. I would like to express my deep gratitude to my senior advisor, **Dr**. **Abdullahi Abu Ibrahim**, for his valuable time, guidance and encouragement. Invaluable feedback and fruitful discussion throughout my preparation hypothesis. I would like to express my thanks and appreciation to Mr Hamzah Marhoon / Al-Esraa University College in Iraq. I must extend my sincere thanks to my advisor. during my research. Thank you to my institution, the Federal Integrity Commission, for their support in completing this project. Finally, I would like to extend my sincere thanks and gratitude to family and friends, especially Support and encouragement for me without whom I would not have completed my studies. **Special dedication:** Every challenging work needs self-effort too as a guide for the elderly, especially those who have been very close to our hearts. My humble effort I dedicate to my father's soul Dr. Mohammed kadhim kamal Al-Attar And to the loving heart of my mother with encouragement and Day and night prayers make me able to get it and to my brothers and sisters and all my family members for their support for me during the study period This success and honour Along with all the hard work and respect.

ABSTRACT

DESIGN AND ENHANCEMENT OF MICROSTRIP PATCH ANTENNA FOR PERSONAL NETWORKS IN THE GOVERNMENT INSTITUTIONS

Al-Attar, Saif

M.Sc., Electrical and Computer Engineering, Altınbaş University,

Supervisor: Asst. Prof. Dr. Abdullahi Abdu IBRAHIM

Date: August/2022

Pages: (75)

In our daily lives, especially in the past few years, wireless communications have become an important and effective era in performing tasks and communicating wirelessly without the need for a physical medium. The most important feature of remote communications is the ease of use and installation in places where it is difficult to communicate physical media, and the possibility of sending information over large distances by employing electromagnetic waves. With this rising in the number for the appliances and the implementations connected to the wireless network, there has been crowding, which negatively affected the speed of data transmission. One of the effective solutions proposed by network operators is to switch to the use of high frequencies to meet the users' desire for high data transmission speed. The antenna is considered as a one of the considerable essential elements in the wireless communication systems. The microstrip antennas are one of the types of antennas used, but they suffer from weak gain and narrow bandwidth, so there is an importance to improve these parameters. In this paper, a teeny sized MPA is simulated and optimised to be operated at the 62 GHz frequency for the personal network applications within the government institutions based on the CST antennas modelling software. In order to improving the MPA performance, two shapes of the Frequency Selective Surface (FSS) are used. The FSS is acting as a passive filter to make the antenna more intelligent because it is selectively passing the preferred frequencies or rejecting the unwanted ones.

Keywords: Antenna, CST, FSS, Indoor communications, Government institutions.

TABLE OF CONTENTS

Page

LIST OF TABLES

Page

LIST OF FIGURES

Page

ABBREVIATIONS

mm-waves	:	Millimetre Wave
RF	:	Radio Frequency
GPS	:	Global Positioning System
EHF	:	Extremely High Frequency
ITU	:	International Telecommunication Union
WIGIA	:	Wireless Gigabit Alliance
HD	:	High Definition
AM	:	Amplitude Modulation
FM	:	Frequency Modulation
MPA	:	Microstrip Patch Antenna
FSS	:	Frequency Selective Surface
EBG	:	Electromagnetic Band Gap
AC	:	Alternating Current
HPBW	:	Half Power Beam Width
FNBW	:	First Null Beam Width
RL	:	Return Loss
VSWR	:	Voltage Standing Wave Ratio
MAs	:	Microstrip Antennas

1. GENERAL INTRODUCTION

This chapter illustrates at a glance a general introduction about the wireless communications, millimetre wave (mm-waves), mm-waves properties, and mm-waves applications. Also, in the chapter the literature survey, the problem statement, the thesis objectives will be presented as well.

1.1 INTRODUCTION

Due to the importance of the wireless communication in many of the vital applications is considered as an impactful technology in the modern decade contributing a decisive influence on the way of the human life. Whereas working via distance, online gaming, factories monitoring, offices management, and other activities that interact with people and the world, all of the mentioned are done via the help of wireless communications. In addition, there are billions of the cell-phone backers around the globe, and a broad variety of devices in addition to the mobile phones utilises the cellular technology to doing their connectivity. With the modern growth in the wireless communications, the Wi-Fi technology was embedded with numerous appliances such as smart mobile phones, computers, smart cars, drones, kitchen machines, smartwatches, and a lot of modern applications [1], [2].

Besides that, the satellite communication systems are employed to support the video or the voice transmission and data applications for receivers covering the earth, in the air, and the in space. More specifically, the wireless communication can be interpreted as the transmission of the signals that are carrying the data amidst a pair or more further nodes that aren't linked by the wire conductor. The variety of the available wireless technologies are tended to use the Radio Frequency (RF) wave. Besides the RF waves, the distances could be small, like a some of the meters for the television or as far away as many thousands or exact several of the kilometres for the applications of the deep-space. The wireless technologies contain various kinds of firm, roving, and hand-held implementations, such as the two-way radios, the cellular telephones, the personal digital assists, and the wireless networking. The further illustrations for the application of radio technologies incorporate the GPS systems, the controlling for the garage door, the wireless computer peripherals, the radio receivers, the satellite television, and the cordless phones. Figure 1.1 illustrates the interaction between the various of the appliances within the wireless communication network [3], [4].

Figure 1.1: The organization for wireless communication network [4].

1.2 COMMUNICATIONS VIA MM-WAVES

The millimetre wave (mm-wave), which is additionally recognised as a millimetre frequency band, is part of the frequency spectrum having a wavelength in the range of 10 mm for the lowest point regarding the band (i.e., 30 GHz) and 1 mm for the highest point regarding the band (i.e., 300 GHz). This frequency band is also recognised as the Extremely High Frequency (EHF), this term is allocated through the International Telecommunication Union (ITU). Because of the short wavelength that is characterised by the mm-wave, antennas of the wireless system will be in compact physical dimensions [5].

The mm-wave frequency bands are presently attracting more of the investigators' attention due to the offering of the huge bandwidth that is contributing a large data rate for the wireless communication tools. According to the mentioned benefit, the mm-wave will be considered as a pioneer for many of the applications such as the wireless transfer of high-definition television and the ultra-high-definition video [6].

The mm-waves comprise the E-band and the V-band that are together the couple key bands in this part of the spectrum. The V-band can be considered as an uninterrupted spectrum from which take a range of 57-66GHz; while the E-band are ranging from 71-76 and 81-86 GHz [7], as shown in Figure 1.2.

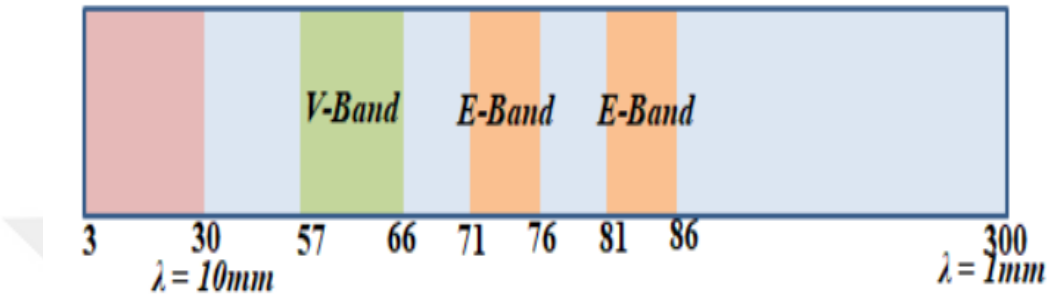

Figure 1.2: The frequency spectrum for the mm-waves [7].

The more extended transmission ranges could be achieved via utilising the E-band as it offered large data rates and less oxygen assimilation as compared with the V-band, as demonstrated in Figure 1.3 [8].

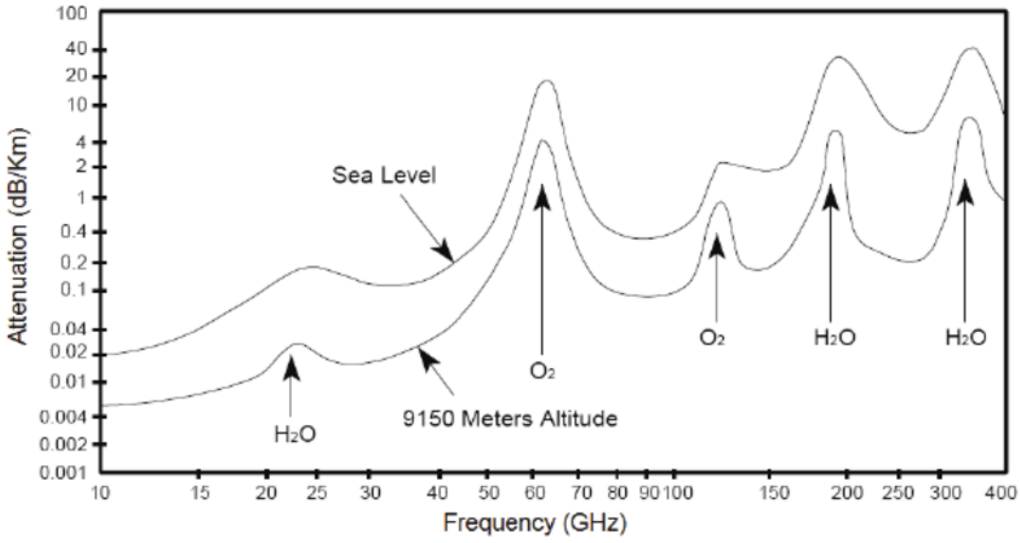

Figure 1.3: Oxygen absorption for the frequency range of 10-400GHz [8].

In general, the mm-wave frequency band can be practised in many of the vital applications some of which can be summarised as following:

a) Virtual Reality
b) Wireless Communications
c) Wearable appliances
d) Personal networks
e) The future of 5G communication
f) Satellite Communications
g) Object imaging and tracking

The junior and current employment of the mm-waves are exhibited in Figure 1.4. These employments comprise the: IEEE 802.11ad WiGig, satellite transmission, automotive, radar, 5G and tiny cell approach, medical applications like mm-wave therapy, body scanning, virtual reality headsets, and HD video transmission [7], [8].

Figure 1.4: Some of the mm-waves applications [7].

The utilising of the mm-waves provides the users/manufacturers many advantages some of which are: large bandwidth, small components size, higher resolution, slight interference and enhance the security [9].

1.3 LICENSE FREE FREQUENCY BAND

As previously above mentioned the V-band or the 60 GHz wireless frequency is a portion of the mm-waves band. An essential qualification in the difference of the frequency bands, there is two essential distribution the first one users need a license to reach it the AM and FM broadcasters. While the second kind is doesn't require a license to reach it, this called unlicensed operation. The unlicensed frequency band is different from one country to another [9], this depends on the criteria and the rules in such countries, as demonstrated in Figure 1.5.

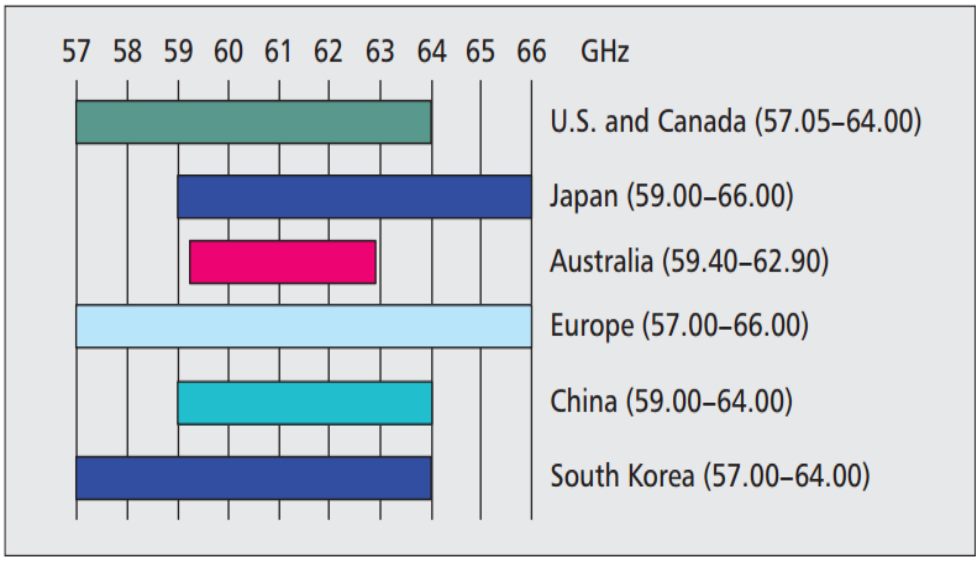

Figure 1.5: The license-free frequency band for 60GHz [9].

This band is unique in its properties, whereas there isn't any other available around the globe unlicensed spectrum that is able to provide 14GHz frequency bandwidth. Such extensive bandwidth allows for the reaching of low-cost gigabit data rates with a free license operation. Such the Wi-Fi or the Bluetooth; the 60GHz (i.e., V-Band) tools can be expanded as required without the needing for the licensing that provided by the regulatory companies or the government. Such liberty option grants the ability to implement a cost-effectively and swiftly expand for the V-Band wireless services [10].

1.4 PERSONAL NETWORKS

The personal network is a kind of available network arrangement responsible for the exchange of data within the indoor range (i.e., vicinity of the person). In general, such of these systems are usually installed/designed to operated wireless. The personal network involves the transmission of information or data between a variety of available appliances such as smartphones, computers, tablet computers, and other fixed or portable applications, as demonstrated in Figure 1.6 [11].

Figure 1.6: Arrangement of the personal network in the government institutions.

Besides the development of the technology and the scientific field that contributes large trends for the innovations in the research area toward the evolution of wireless communications networks for the personal networks. Many of the investigations for the utilisation of the V-band from the mm-wave in the license-free spectrum are still not mainstream. The principal interest for network developers and vendors is the unfavourable propagation characteristics for the mentioned frequency band due to its short wavelength and the requirements for the high directionality, which renders the V-band links extremely weak against the blockage and mobility. Nevertheless, the

appearance of the multi-band chipsets prepares the feasibility for the leveraging of the most known and robust Wi-Fi technology to support the 60GHz band in order to produce seamless with many of the Gbps connectivity [12].

1.5 PROBLEM STATEMENT

Besides the requirements of reaching a high data rate transmission and minimising of the data congestion in personal networks that are employed in the government institutions to facilitate the work of employees, the utilising of the license-free frequencies is an effective and good solution to solve the problems that are previously mentioned. Because of the obvious advantages that are offered by the Microstrip Patch Antenna (MPA) such as low fabrication cost, ease of fabrication, and low profile, the MPA is commonly used in many wireless communication applications (e.g., personal networks). However, the principal limitations for the traditional MPA are poor gain and narrow impedance bandwidth for various wideband wireless communication services. So, there is a need to optimise the mentioned parameters of the MPA.

1.6 STUDY OBJECTIVES

This work is introduced to solve the problem statements that are previously declared in the prior section. So, the contribution of this study can be reviewed briefly as follows:

a) Design, analysis, simulation, and enhancement of an MPA functioned at the 62 GHz that is selected for the utilisation within the personal networks (i.e., indoor applications) for government institutions and in the future of the next generation of wireless communications.
b) Enhancement of the performance of the proposed antenna by employing the frequency selective surface (FSS) which will be declared in the next chapter.

1.7 LITERATURE SURVEY

Several studies have been conducted in the past regarding the use of an unlicensed frequency spectrum for the personal networks. In addition to that, many studies and works have been conducted to improve the performance of microstrip antenna, below some of which will be reviewed:

a) In this previous study, the authors of the article [13] have been designed and simulated of a small-sized wideband MPA. The authors were used the inset feed scheme to get the optimum coupling between antenna and source. The Simulated MPA was introduced to be operated for the un-licensed band for the frequency of operation 60GHz. In addition, the authors have been etching slots inside the antenna patch in order to enhance the gain, bandwidth and the efficiency of the simulated MPA.
b) In this work, the authors have been placing the basis for the graphene-based MPA to function in three frequency bands, which are considered promising for eventual wireless communications. The graphene material possesses abnormal features one of the most important in the electronic area is the variated electric conductivity which changed as desired. The authors have used graphene as inserted slots within the MPA patch to attune the resonant frequency of the MPA by increasing or reducing the graphene chemical potential. The proposed MPA have functioned at the 300 GHz, 350 GHz, and 410 GHz bands, of the mm-wave band [14].
c) In work, the authors have been designed, simulated, and manufactured a small and MPA array for 60GHz purposes. The MPA array is often utilised to improve both of the gain and the frequency bandwidth. To ensure getting the best performance the array was fed concurrently by using a parallel/series feed jointly with the differential feeding technique. The manufactured MPA array achieves operation bandwidth (S11 < -10 dB) from 55 to 68 GHz, which meet with the worldwide 60-GHz licensed free band [15].
d) In this article, the researchers have been presented a pair of the practical realization illustrations for the MPA at 28GHz and 60GHz. The simulated antennas were made up from a copper patch, ground plane, substrate, and feds via the quarter-wave line feeding approach. The researchers have been described the challenges and the restrictions that they faced during the design procedure and the conciliating of antenna performance specifications as well as the fabrication [16].
e) In this article, the researchers have been made a low profile single MPA and MPA array based on the enhancement approach named as mushroom-like EBG organization for the 6-GHz uses. This approach was used to eliminate the impression of the surface wave that is normally noticed as undesirable, whereas it leads to an increase in the level of the side lobes, and minimise the MPA gain and efficiency. This problem can be addressed by

employing the EBG structures to suppress the effects of such waves. The organization of the proposed MPA was comprised of a substrate, ground plane, and the patch surrounds it mushroom cells were introduced. Following that, the researchers have been examined the proposed MPA performance after adding the mushroom cells and they noted enhancements in the side lobes level to be −16.5 dB instead of −6.8 dB, the MPA directivity was improved to 10 dBi instead of 5.77 dBi, and finally, the MPA efficiency has been improved to 95% instead of 80% by practising the EBG with the proposed MPA [17].

1.8 THESIS ORGANISATION

This thesis is made up of four fundamental chapters, the organization and the outlines of the each consequent chapters are presented as following below:

a) Chapter Two

This chapter of the thesis deals with providing a detailed and complete explanation about the basic parameters of antennas and MPAs, their advantages and disadvantages, their types and feeding methods, in addition to the basic methods for their analysis.

b) Chapter Three:

This chapter of the thesis demonstrates the necessary steps for the proposed antenna configuration designs and also exhibits the acquired outcomes after doing the simulation procedure in the antenna analysis software.

c) Chapter Three:

This chapter demonstrates concludes from introducing this work and the possible additions or modifications to develop this work in the future by the researchers and students.

2. ANTENNA FUNDAMENTALS

In this chapter of this thesis, we will address several sub-parts, which can be summarized by the antenna fundamental parameters, microstrip antennas, and mushroom like electromagnetic bandgap.

2.1 ANTENNA ESSENTIAL PARAMETERS

This section of the thesis covers the antenna essential parameters such as antenna regions, antenna radiation pattern, antenna directivity, antenna gain, antenna return loss, antenna bandwidth, antenna equivalent circuit, and the efficiency of the antenna.

2.1.1 Antenna Regions

When a high-frequency current is passed through an antenna, it causes it to produce an electromagnetic field in the space around it that has a correspondingly high frequency. The detailed structure of this field is typically fairly complex, and it is highly dependent on the design of the antenna. When it comes to the electric and magnetic fields close to the antenna, there is practically nothing that can be said about them without resorting to complex numerical calculations. The only exceptions to this are a few straightforward examples. As we get further away from the antenna, the field starts to take on the appearance of spherical waves, which is a positive development. The greater the degree to which the waves resemble spheres, the further apart they are. Spherical waves are especially helpful due to the fact that many of the calculations can be done with relatively straightforward equations. As depicted in Figure 2.1, Typically, the area wrapping the antenna is partitioned into three distinct regions that are referred to as antenna regions [18]:

a) The reactive near-field region: This region instantly surrounds the antenna and is where the majority of the reactive field can be found. The electric (E) and the magnetic (H) fields aren't needed in phase besides the each other, and the angular field dispersal is positively dangling on the distance and direction from the antenna. The E and H fields can also be out of phase with each other. It is possible to conceptualize it as a reactance that is tasked with preventing the loss of energy while simultaneously storing it.
b) The region referred to as the radiating near-field (Fresnel): This zone is located all around the reactive near-field region that was expressed earlier. Within this region, the radiation

fields prevail, the electric and magnetic fields are in phase, despite the allocation for the corner field is still determined by the means of the stretch from an antenna.

c) This region surrounds the reactive and radiating near-field regions that were represented earlier. It is indicating to like the far-field or as the Fraunhofer region. It reaches into endlessness and is a representation of the extended maturity of the space that the wave typically moves through. In this region, all of the fields are able to radiate, the dispersal of the angular field is practically separated from the distance from the antenna, and it is possible to make an approximation of it using spherical wavefronts. Because it is so far away from the antenna, its dimensions and shape are of little consequence any longer, and we can treat it as though it were a point source instead.

The previously illustrated regions are helpful for identifying the field configuration in order to determine which simplifications can be utilized; however, there is neither a clear boundary nor a sudden alteration in the field creation.

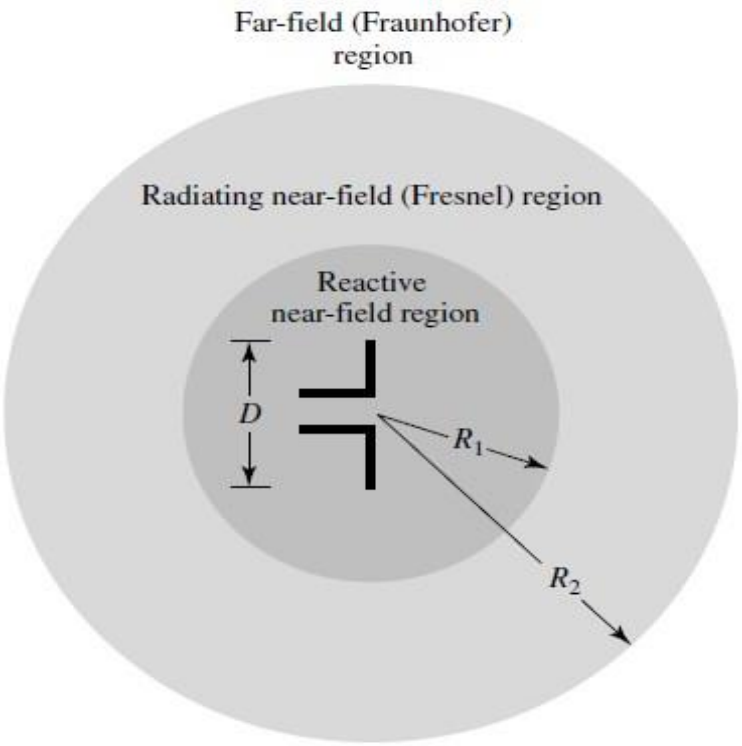

Figure 2.1: Principal regions of antenna [18].

2.1.2 Antenna Radiation Pattern

An antenna is a specialized type of transducer that can convert alternating current (AC) fields into an RF field or the vice-versa. Antennas are used in radio communications. There are a couple of the primary kinds: the antenna in the receiving side, which captures the RF power and supplies AC to an electronic device, and the antenna in the transmitting side, which is feeding AC from electronic devices and generates an RF field. Both types are referred to simply as antennas. The transmission and reception of electromagnetic waves in a certain orientation requires the use of an antenna. Several types of the antennas can be employed for the sending and receiving the various of the signals coming through the distinct directions of the air, while others are used exclusively for one direction. A perfect or the optimum antenna must be efficient at the both of the sending and the receiving for the power in order to be considered one. Additionally, the frequency band of the antenna resonance should ideally be required. A mathematical form or graphical illustration for the characteristic of the antenna as a function of the space coordinates is what is meant when speaking of an antenna's radiation pattern. Commonly, the radiation pattern for the antenna is usually obtained within the far-field zone and is interpreted as a function of the trendel coordinates in this region. The polar graph displays the radiation pattern, which is a two- or three-dimensional representation of the distribution of energy. The radiation pattern is typically normalized before being graphed using decibel (dB) units. The three-dimensional pattern of the radiation field is depicted in Figure 2.2 below. The major lobe, which is also referred to as the main beam, is the region where the most radiation is produced. There are many types of antennas, and some of them have more extra than a couple of the main lobes. The remaining lobes are referred to as minor lobes, and each of these minor lobes could be furthermore subdivided into two parts: side lobes and back lobes. The major lobe and the side lobes are typically neighbouring to one another. The major lobe and the back lobe are at right angles to one another, making a total angle of $\theta = 180^{o}$. The primary objective in the design of a good antenna is to maximize the performance of the major lobe while minimizing the effects of the side lobes on radiation [19].

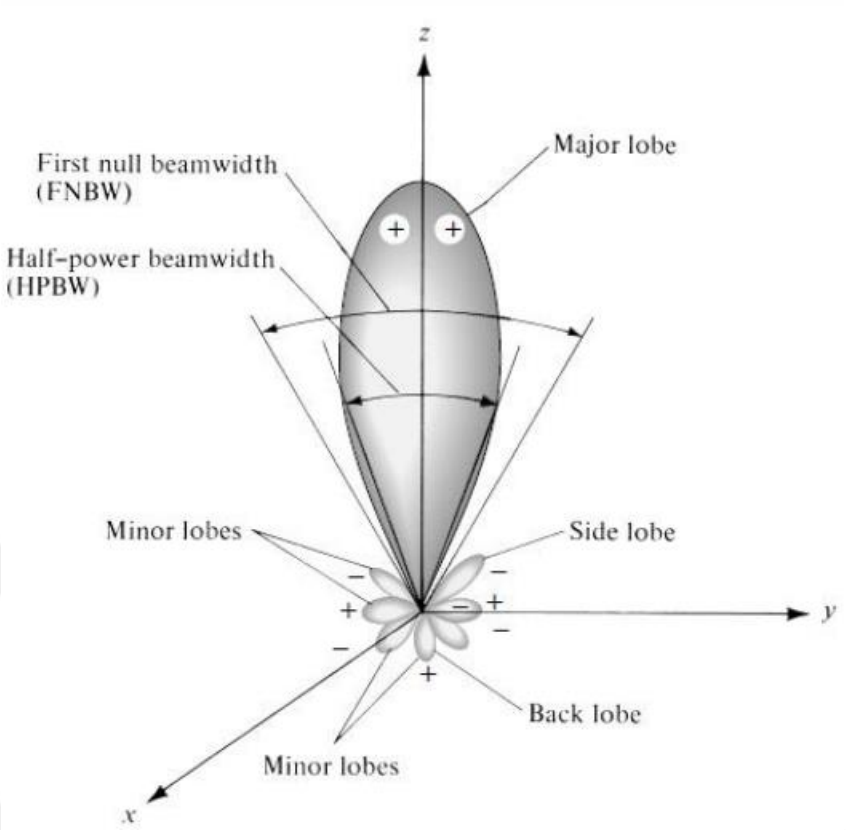

Figure 2.2: General organization of antenna radiation pattern [19].

The beam width can be thought of as the angular distance that separates two points that are exactly alike but are located on the obverse portions of the pattern maximum. There are primarily two different kinds of beamwidths that are employed:

a) Half Power Beam Width (HPBW); and
b) First Null Beam Width (FNBW).

The IEEE defines the term HPBW, as follows: The angle that exists between the two directions in which the radiation intensity is equal to the one-half value of the beam is the same in a plane that contains the direction in which a beam's utmost is located. The angular distance that separates the first null of the radiation pattern from the second null is what's known as the FNBW, the power pattern in the 2D mode is presented in Figure 2.3.

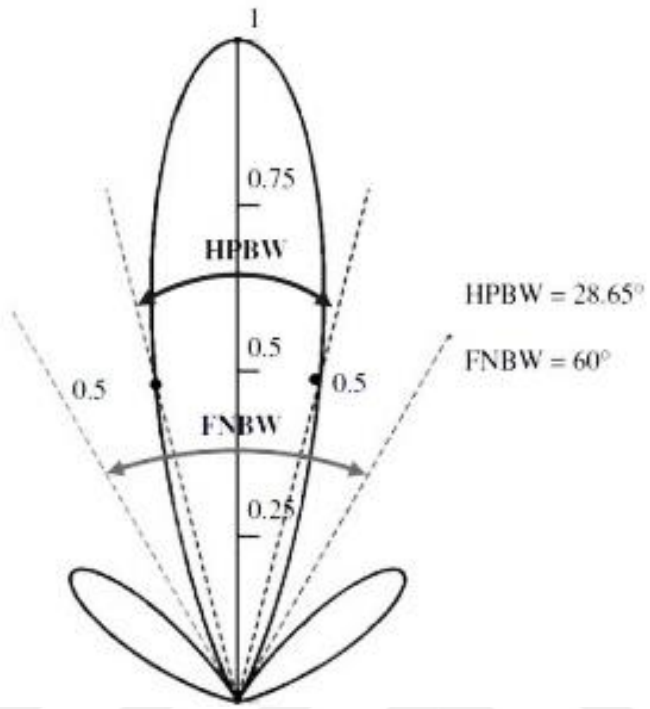

Figure 2.3: The 2D antenna power pattern [19].

2.1.3 Antenna Directivity (D)

The D value of the antenna is depicted as the proportion for the radiation intensity in a certain direction away from the antenna to that averaged out in the other rest directions. The formula for determining the median radiation intensity is as follows: the entire power radiated by the means of the antenna is equal to the entire power divided by 4π. When the direction isn't fixed, the direction in which the radiation intensity is greatest is presumed to be the one that is being emitted. In simple form, the D of the antenna can be expressed in the mathematical form as following [20]:

$$D = \frac{U}{U_o} = \frac{4\pi U}{P_r} \qquad (2.1)$$

Where:

U: is indicate to the radiation intensity for the antenna;

U_o: is indicate to the radiation intensity for the isotropic source; and

P_r: is indicate to the radiated power from the antenna.

2.1.4 Gain of Antenna (G)

The capacity of the antenna, in comparison to that of a theoretical antenna, to radiate in any direction to a more significant or more deficient extent is referred to as the antenna's gain. If it were possible to construct an antenna in the shape of a perfect sphere, it would emit radiation in an equal amount in each of the 360 degrees around it. An antenna with these characteristics is referred to as an isotropic antenna in theory, but in practice, there is no such thing. On the other hand, its mathematical model is utilized as a comparison standard for the gain of the practical antenna. Compared to isotropic antennas, omnidirectional antennas naturally have a gain of 2.1 dB in terms of the signal that they are able to radiate. This gain in transmitting horizon distance away from the antenna is achieved by a vertically oriented Omni antenna, and it comes at the spending of the transmitting both above and beneath it. The pattern reminds one of the doughnuts, if that makes any sense. In a general sense, the gain for the antenna could be interpreted and understood to be the proportion of the intensity in a particular direction to the radiation intensity that would be received if the power that was received by the terminals of the antenna were to be radiated as an isotopically pure signal [21].

2.1.5 Return Loss (RL) of Antenna

Antenna RL is a significant merit or parameter when examining the antenna performance. It is associated with the impedance matching and the maximum power transfer principle. RL describes the effectiveness of the power delivery from the source of the power to the antenna. RL is described by the ratio of the incident power on the antenna (P_{in}) to that which returned from the antenna to the source direction (P_{ref}). As the ratio of $\left(\frac{P_{in}}{P_{ref}}\right)$ increased, this is the better and signifies that the power actually accepted via the points (i.e., terminals) of the antenna is more than the reflected power back to the source, the return loss can be expressed mathematically as follows [22]:

$$RL = 10log\left(\frac{P_{in}}{P_{ref}}\right) \quad (dB) \tag{2.2}$$

Generally, one of the considerable widely utilized parameters in the design of the antennas is the RL. The reflection coefficient, also known as the RL, is a measurement that indicated the quantity of power that is reflected from the antenna.

2.1.6 Antenna Bandwidth (BW)

The BW of the antenna is one of the important things that should be focused on when designing the antennas. The BW of the antenna indicates the band of the frequency bands through which the antenna able to be operated properly. The antenna's BW is the number of the frequencies for which the antenna will manifestation a VSWR in the range of 2:1. The BW can also be represented mathematically as a percentage for the center frequency of the band, as follows [23]:

$$BW = \frac{f_H - f_L}{f_c} \tag{2.3}$$

$$B_r = \frac{f_H}{f_L} \tag{2.4}$$

Where:

f_H: indicates to the highest boundary frequency in the BW;

f_L: indicates to the lower boundary frequency in the BW;

f_c: indicates the center frequency of the BW; and

B_r: indicates the ratio BW.

In the case of the B_r is greater than or equals 2, then the antenna is covering a broadband of the frequency and otherwise the antenna is classified as a narrow bandwidth. The method to estimate how the antenna operates correctly at the required frequency band is by calculating it's $VSWR$ or return loss. Practically in the antenna design, the BW can be obtained from the RL pattern. In the case of the RL less than or equals (-10 dB) this leading to obtain a reasonable performance. So, to measuring the BW of the (-10 dB) cretria is used, in other words, the BW of the antenna is measured at $RL = -10\ dB$, as presented in Figure 2.4.

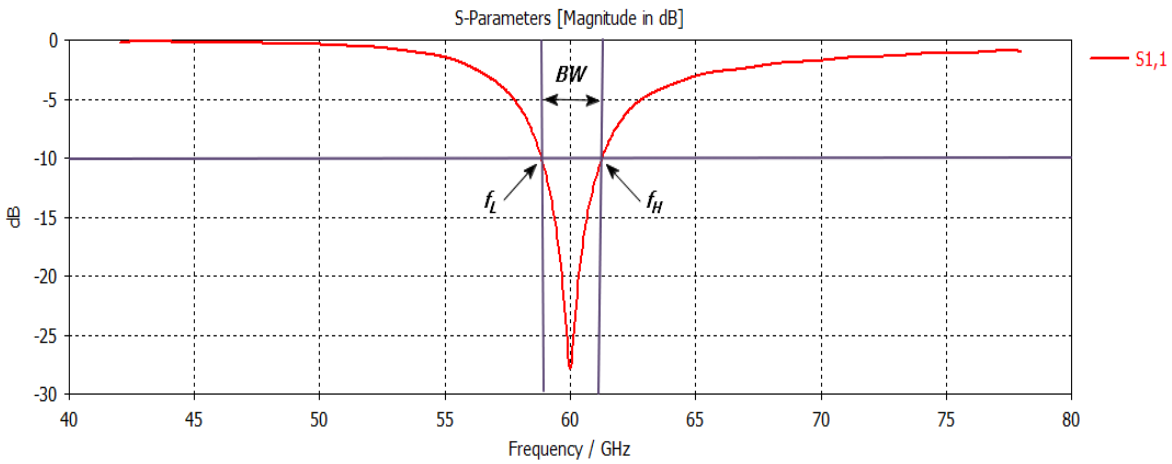

Figure 2.4: Measuring of the antenna bandwidth from return loss plot.

2.1.7 Antenna Equivalent Circuit

The corresponding circuit for the transmitting antenna is shown in Figure 2.5. The radiation resistance R_r and the loss resistance R_L are the two categories for the resistive portion for the antenna impedance. The total power that is radiated by the means of the antenna is the power that is actually lost in the radiation resistance. This power is indicated to as the "radiation power". The loss resistance, on the other hand, is the power that is wasted by the means of the antenna due to losses in the conducting or insulation components that are made up the antenna [24].

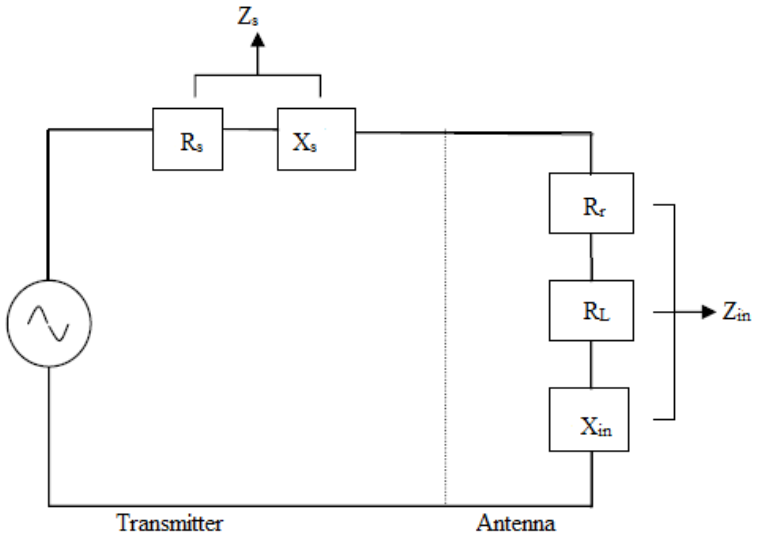

Figure 2.5: Representation of the antenna equivalent circuit [24].

The antenna's input impedance can be characterized in a variety of ways. To begin, an antenna's input impedance can be expressed as the impedance offered by the means of the antenna at its terminals. It's furthermore the voltage-to-current ratio at the two terminals. The proportion for the relevant ingredients of the E-field to that of the H-field at a point this is another method of interpreted the input impedance. As a result, the input impedance is [25]:

$$Z_{in} = R_{in} + JX_{in} \quad (2.5)$$

Where:

Z_{in}: indicate to the total input impedance at the antenna terminals;

R_{in}: indicate to the resistive part of the antenna; and

X_{in}: indicate to the reactive part of the antenna.

2.1.8 Voltage Standing Wave Ratio

The VSWR or can be refer also as the Standing Wave Ratio (SWR). This term can be interpreted as the reflection coefficient which is specified how considerably the power is reversed back from the terminals of the antenna. Additionally, this term can be expressed in the mathematical form through the reflection coefficient (Γ) as demonstrated in the following relation:

$$VSWR = \frac{1 - \Gamma}{1 + \Gamma} \quad (2.6)$$

Usually, the VSWR is varying in the range of $1 \leq \text{VSWR} \leq \infty$, whereas, For the excellent antenna performance the VSWR is close as possible to "1", this signify that there isn't a power is echoed back (i.e., reflected) from the antenna terminals to the source. Antenna with the VSWR in the range 1 and 2 is supposed to be a highly rendering antenna. The reflection coefficient is likewise comprehended as the S_{11}(i.e., the scattering parameters) which demonstrates how much the amount of the power is returned back from the connection points of the antenna to the source of the electric power [25].

2.1.9 Impedance Matching

The transmission line and the microwave links both require a properly matched impedance in order to function properly. An impedance matching connection is introduced to be amidst the load impedance, which is the antenna, and a strip or the transmission line, which is the feeding point.

In the case, this location corresponds to the location amidst the antenna and the line of the feeding. It ought to be lossless in order to prevent any loss of power. With the assistance of the matching circuit, it is possible to prevent loss due to reflection in the transmission line; however, multiple reflections may still take place. Changing the value of the matching networks, which is also referred to as setting, is necessary in order to prevent multiple reflections from occurring [26].

2.1.10 Impedance Matching Significant

The process of matching between the antenna and the source of the electric wave is very important and a reason for making the antenna performance high. Below we explain the importance of the matching process [27]:

a) When the load impedance is matched to the line impedance, utmost of the power is reached, and the power loss because of the reflection that is present in the feeding line is reduced.
b) The single-to-noise ratio of the system's elements, such as the antenna and low-noise amplifier, will be improved by applying the impedance matching network.
c) The impedance matching network will aid in the reduction of amplitude and phase errors in such antenna arrays.

2.2 MICROSTRIP ANTENNAS (MAS)

In this section, after a brief introduction to the MAs, the benefits and drawbacks of using them are discussed. Following that, a number of the feed modeling approaches will be presented and then discussed. In conclusion, a comprehensive explanation of MAs analysing and its theory are presented as well as discussed. In addition, the operating mechanism is broken down and explained.

2.2.1 Introduction

The MAs can be broken down into four distinct categories, each of which is depicted in Figure 2.6. The MPAs, which are the extreme common and widely utilised type, are depicted in Figure 2.7 as having a ground plane on the opposite side of a dielectric substrate that features a radiating patch on one side of the substrate.

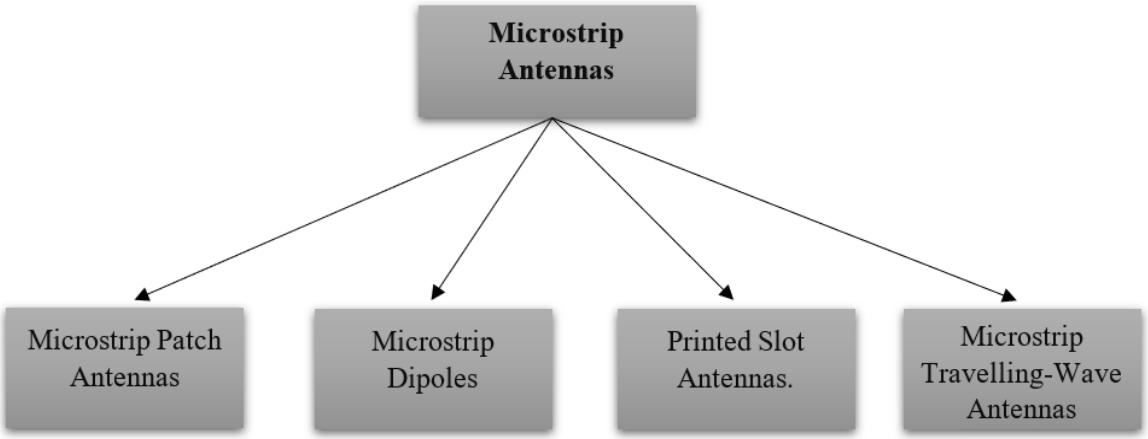

Figure 2.6: The common types of MAs.

The radiating patch, in most circumstances, is constructed through the utilization of a conductive material such as copper, gold, or another, and it can made from any form that is imaginable. On the dielectric substrate, the radiating patch and the powering lines are typically photo-etched to create the desired pattern [28].

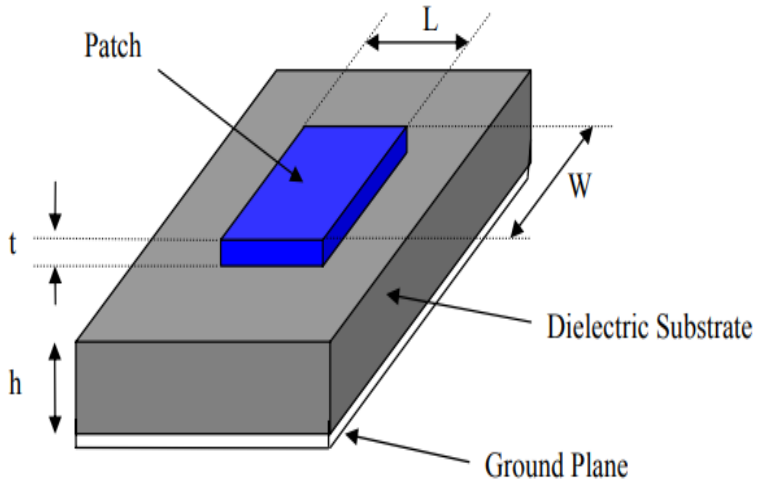

Figure 2.7: Structure of the MPAs [28].

As can be seen in Figure 2.8, the patch is typically in one of several standard shapes, such as a square, rectangular, circular, triangular, or elliptical, in order to make the analysis and prediction of the performance as straightforward as possible. In the case of the rectangular shape patch with the length L of the patch is typically expressed as $(0.3333\lambda o < L < 0.5\,\lambda o)$, where (λo) is the

wavelength of the air medium. The size of the patch has been purposefully selected to be quite small so that ($t << \lambda o$) (whereas the t is indicated to the patch thickness). In most cases, the thickness h of the dielectric substrate will be ($0.003\lambda o \leq h \leq 0.05\lambda o$). The constant for the dielectric of the substrate, denoted by the symbol of ε_r, which is typically found to fall somewhere in the value of ($2.2 \leq \varepsilon_r \leq 12$).

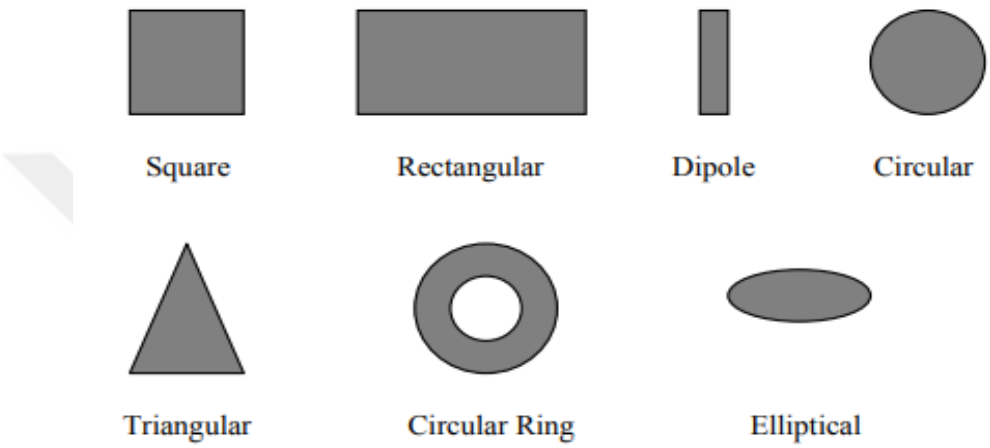

Figure 2.8: Popular used shapes for the patch [28].

The fringing fields that exist amidst the edges of the patch and the ground plane are the essential reason that MPAs are able to radiate. The stout or the solid dielectric substrate with a small dielectric constant is desirable for pretty antenna rendering because it offers better efficiency, more extensive BW, and better radiation. This is because of the low dielectric constant. On the other hand, this configuration results in a larger size for the antenna. Higher dielectric constants are required for the designing of the compact MPA; however, this results in a reduction in efficiency as well as a narrowing of the antenna's bandwidth. Because of this, it is necessary to find a middle ground amidst the total dimensions for the antenna and its rendering of the antenna [28].

2.2.2 Advantages and Disadvantages

As a result of the MPA's low-profile design, it is becoming an increasingly popular choice for use in wireless applications. As a result, they are an excellent choice for the embedded antennas found in the strolling and the handheld wireless appliances such as the mobile phones, the pagers, and the other similar implementations. These antennas used for telemetry and communication on missiles typically take the form of microstrip patch antennas because of their thinness and

conformability requirements. Satellite communication is another area where they have proven to be useful and successful applications. The following is a list of some of their most significant advantages [29]:

a) Light in weight and taking up small installing space
b) Configuration with a low profile and a planar shape that can easily be designed to be conformal with the instrument surface
c) Low cost to manufacture; as a result, it is possible to produce it in large quantities.
d) Another advantage of this type of antennas are that it can be easily designed and manufactured by researchers, hobbyists as well as manufacturers
e) These types of antennas can support both of the linear or the circular polarization and in some extents the designers can design antennas capable to support the both together
f) Integration with microwave integrated circuits is a breeze for it to accomplish by the utilizing of the MPAs
g) Having the ability to operate at dual as well as triple frequencies
h) Robust in terms of the mechanical structure in the case of the situated on rigid surfaces

With many of the benefits and characteristics that were mentioned previously, on the other hand, there are many of the disadvantages to this type of the antennas, which can be listed as follows [29], [30]:

a) Narrow BW
b) Small efficiency
c) Poor Gain
d) Superior radiation through the strip and connections
e) Terrible end-fire radiator, besides the exemption of the tapered slot antennas
f) Low power treating capability
g) Excitation caused by surface waves

The MPAs have an antenna quality factor that is exceptionally high (Q). A high Q depicts the losses that are associated with the antenna, and a narrow bandwidth and low efficiency are the results of having a high Q. Increasing the thickness of the dielectric substrate is one way to bring down the value of Q. Nevertheless, as the height of the material grows, a proportionally larger

amount of the total power delivered by the source is transferred into a surface wave. Because it is eventually dispersed at the dielectric turns and rationales a degradation of the antenna characteristics, this surface wave contribution can be counted as an unwanted power loss. The use of photonic bandgap structures, on the other hand, can significantly reduce the impact of surface waves. In the case of the utilising the array arrangements for individual elements, it is possible to circumvent other challenges, such as a lower gain and a lower capacity for handling power [30].

2.3 POPULAR FEEDING APPROACHES

The MPAs can be fed by employing the variety of the available and possible methods. Such methods usually classified into two fundamentals categories; the first one is called the contacting technique, whereas the second one is called the non-contacting. In the case of the using of the contacting methods, the radio frequency power is feeds to the terminal of the antenna radiated patch by means of utilizing the connecting segments like as the printed on the same dielectric microstrip line. In the second category, also known as the non-contacting method, the radiation coupling, also known as the electromagnetic field coupling, is utilised to carrying the power from the strip line to the radiating patch. This method falls under the non-contacting subcategory of the approach. The strip line, the coaxial probe (both sorts are considered as a contacting types), the aperture coupling, and the proximity coupling are the four types for the feed strategies that are used the most frequently (both non-contacting schemes). The classification, as well as the various types of feeding methods that are most commonly used, are shown in Figure 2.9 [31].

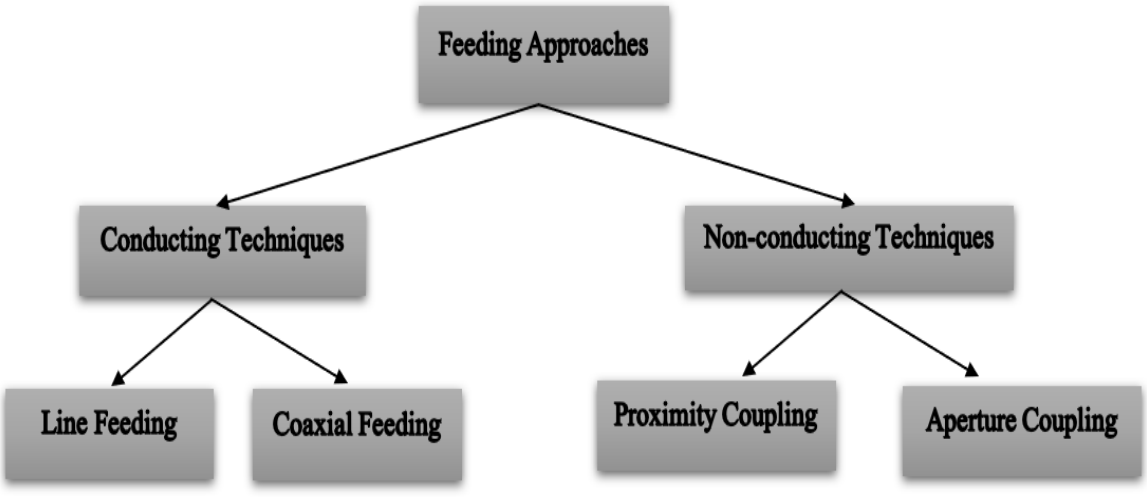

Figure 2.9: Classification of the most known feeding methods.

2.3.1 Microstrip Line Feeding

As can be seen in Figure 2.10, one sort of the feeding strategy involves connecting a conducting strip straight to the one of the edges of the microstrip patch. In comparison to the patch, the width of the conducting strip is significantly narrower, and this particular type of feed arrangement has the distinct advantage of being able to etch the feed over the same antenna substrate in order to produce a planar arrangement [31].

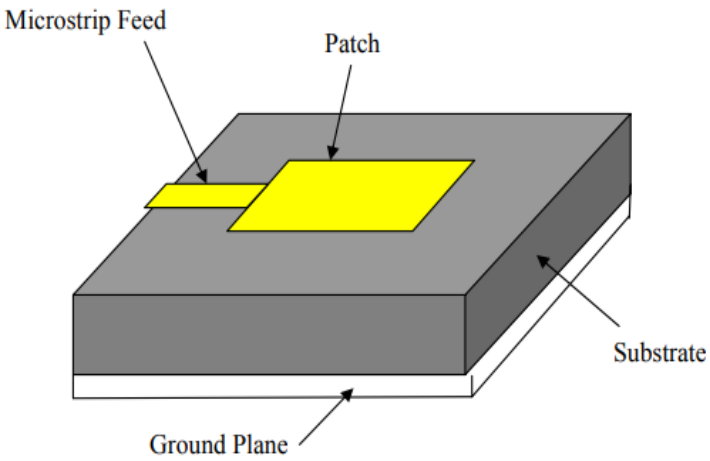

Figure 2.10: Microstrip line feeding [31].

The inset small shear in the patch has been designed with the intention of making it unnecessary to use any other kind of matching element in order to matching the impedance for the strip line to that of the patch. This is accomplished by exercising the necessary control over the position of the inset. The ease of fabrication, the simplicity of modelling, and the ease of impedance matching all contribute to the fact that this is a straightforward feeding strategy. The surface waves and the extra radiation from the feeding both increase as the height of the dielectric substrate that is being utilized gains. This has the effect of reducing the BW of the antenna. Radiation from the feed source also results in radiation that is cross-polarized, which is undesirable [31].

2.3.2 Coaxial Feed

The coaxial feeding, also commonly interpreted as the probe feeding, is a method that is frequently utilized for the purpose of feeding MPAs. Figure 2.11 demonstrates that the core of the conductor of the coaxial connector passes via the dielectric and is then it is soldered with the radiated patch.

In contrast, the ground plane is connected to the conductor that is located on the outside of the connector that commonly called as the sheath [32].

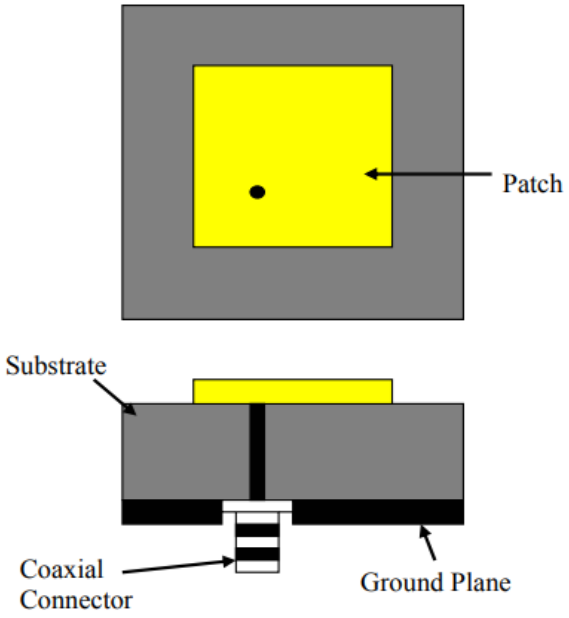

Figure 2.11: Coaxial feeding for rectangular MPA [32].

The fact that the feeding can be situated on any establishment within the radiated patch that the user chooses in order to matching amidst the patch's input impedance is the primary benefit of this particular classification of feeding scheme. This method of feeding produces little to no dummy radiation and is simple to fabricate. It is also intractable for the modelling, this because a puncture required to be prepared in the substrate, and the connector emerges outgoing of the ground plane, which prevents it from being entirely planar for the thicker substrates with ($h > 0.02\lambda o$). On the other hand, its primary drawback is that it offers a narrow bandwidth, and it also requires drilling a hole in the substrate. In addition, for substrates that are thicker, an increase in length of the probe causes the input impedance to become supplemental inductive, which causes troubles with the matching. As was seen in the previous section, both the strip powering line and the coaxial feed have a number of drawbacks when applied to a thick dielectric substrate, which offers a broad BW. These issues can be resolved by using the non-contacting feed techniques that have been covered in the previous section [32].

2.3.3 Aperture Coupled Feed

As can be seen in Figure 2.12, the ground plane acts as a barrier amidst the radiating patch and the strip feeding line that is utilized in this type of the feeding strategy. The coupling that connects the patch to the feed line is accomplished by cutting a small manhole or aperture into the bottom of the ground plane [33].

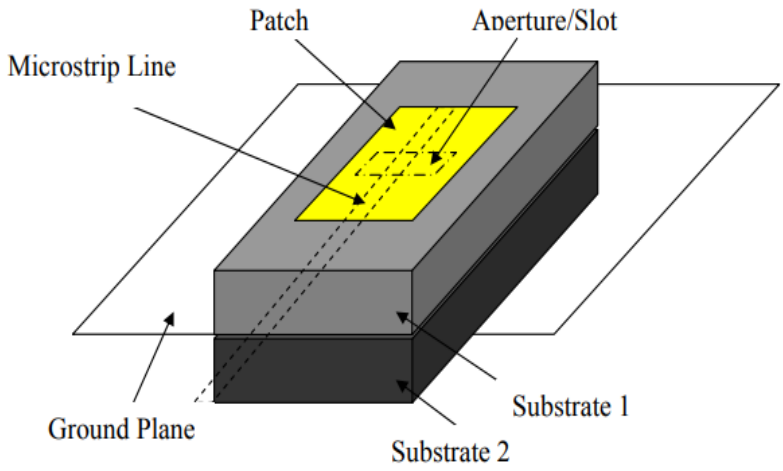

Figure 2.12: Aperture-coupled feed [33].

In most cases, the coupled aperture is cantered beneath the patch. This placement makes the configuration more symmetrical, which in turn results in less cross-polarization. The aperture's form, dimensions, and location all play a role in determining the amount of coupling that occurs between the feeding line and the patch. Whereas, the patch and the feeding line are kept physically separate by the ground plane, which helps to reduce the amount of spurious radiation. In order to maximize the amount of radiation that is emitted by the patch, it is common practice to use a material with a high dielectric constant for the base (i.e., lower) substrate while the thicker material with a smaller dielectric constant is utilised to be for the upper substrate. The fact that this feed technique requires multiple layers, which results in a risen in the whole thickness of the antenna, makes it complicated to be fabricate, which is the technique's primary drawback. In addition, a narrow bandwidth is provided by this feeding strategy [33].

2.3.4 Proximity Coupled Feeding

This particular method of feeding animals is sometimes referred to like the electromagnetic coupling strategy. A couple of a different dielectric substrates are utilised in this design, as can be seen in Figure 2.13. The feeding strip line is placed in the space between the substrates, and the radiating patch is placed on top of the upper substrate. Because of the complete rise in the thickness of the MPA, this feeding technique offers very large BW (as high as 13 per cent), which is the primary benefit. In addition, it eliminates spurious feed radiation, which is another advantage. This strategy of the feeding also supplied an option for two distinct dielectric medium, the first one is for the patch while the second one is utilised for the feeding strip line, in order to improve the rendering of each component individually [34].

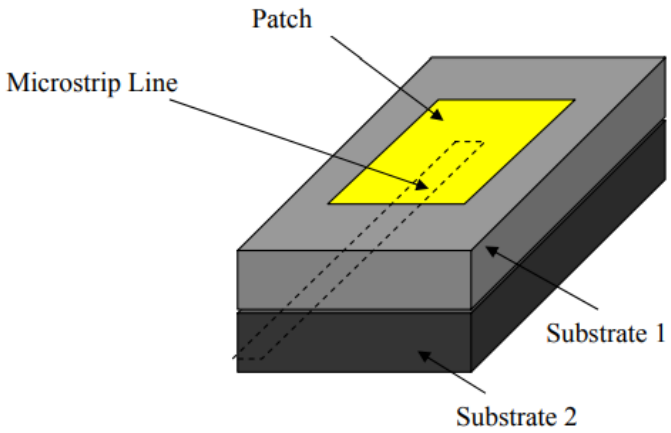

Figure 2.13: Proximity-coupled feed [34].

Through the controlled by the total length of the feeding line and the width-to-line proportion of the patch are two important factors to consider when attempting to achieve matching. The fact that these two dielectric layers need to be properly aligned makes this feed scheme particularly challenging to fabricate, which is the feed scheme's most significant drawback. In addition to this, there is a general risen in the total size of the antenna [35].

2.4 METHODS OF ANALYSING

The farthest communal strategies that are employs for the modelling and the analyses of MPAs can be listed as following [36]:

a) The transmission line model.
b) The cavity model; and
c) The full wave model.

The strip line representative is the most straightforward of them all, and while it does provide some useful insights into the physical world, it is also the least delicate. The cavity modelling for the antenna is further delicate and provides valuable substantial shrewdness, despite the fact that it is inherently complicated. The full-wave strategy is especially authentic, multilateral, and able to treating just single elements, finite and infinite arrays, stacked elements, arbitrarily shaped elements, and coupling. Full-wave models can also treat arbitrarily shaped elements. These models are significantly more difficult to understand and provide significantly less insight corresponded to the previous two models discussed.

2.4.1 Transmission Line Model

In this strategy of the analysing the MPA is expressed in this model by two slots with dimensions of the width of W and the height h, which are kept apart by a strip line with length L, as demonstrated in Figure 2.14. The microstrip is practically a line that is not homogeneous and is composed of two dielectrics. These dielectrics are typically air and the substrate.

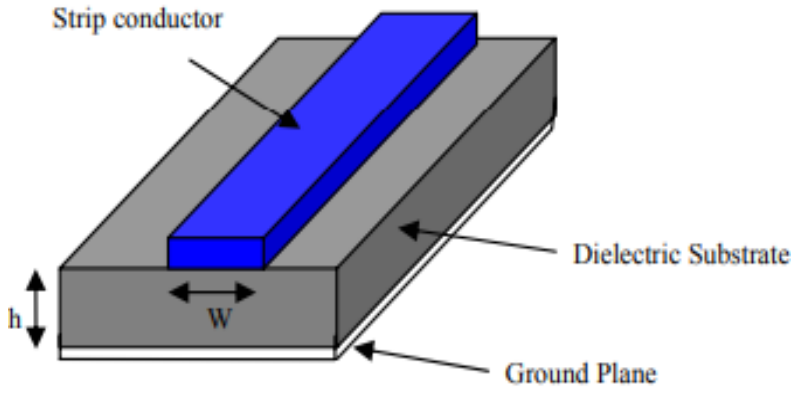

Figure 2.14: Microstrip line [36].

As a result, as can be deduced from Figure 2.15, the plurality of the E-field lines is located in the substrate, while some portions of other lines are located in the air. Because of this, the transmission

line in question is not capable of supporting the refined transverse electric-magnetic mode of transmission due to the phase velocities in the free-space and the substrate would be very distinct from one another. Alternately, the quasi-TEM mode would end up being the most important mode of the propagation. Therefore, in order to account for the fringing and the wave propagation in the line, it is necessary to obtain a value for the effective dielectric constant, which is denoted by ε_{reff}. Due to the fringing fields, almost the perimeter of the patch isn't encompassed in the dielectric substrate but is also distributed in the air, commonly the value of ε_{reff} is slightly less than ε_r. This is because Figure 3.8 shows how the fringing fields are spread out in the air. The expression for ε_{reff} is given as [37]:

$$\varepsilon_{reff} = \frac{\varepsilon_r + 1}{2} + \frac{\varepsilon_r - 1}{2}\left[1 + 12\frac{h}{W}\right]^{\frac{-1}{2}} \tag{2.7}$$

Where:

ε_{reff}: indicate to the effective dielectric constant

ε_r: indicate to the constant of the dielectric of the MPA

h: indicate to the thickness of the substrate

W: indicate to the width of the patch of the MPA.

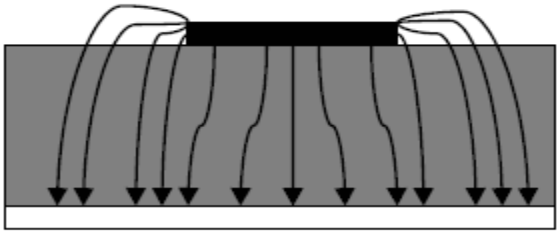

Figure 2.15: Electric field lines [37].

Consider the shown Figure 2.16, which depicts a microstrip patch antenna that is rectangular in shape and rests on a substrate that is taller than it is wide. The length of the antenna is "L" and the width is W. We have chosen the coordinate axis in such a way that the length will run straight the x-direction, the width will run straight the y-direction, and the thickness or the height will run along the z-direction.

The length of the radiated patch needs to be somewhat less than 0.5λ, where the λ is indicates to the wavelength within the dielectric medium and is equals to $\lambda o/\sqrt{\varepsilon_{reff}}$, where λo is the wavelength in free-space in order for it to operate in the principal (TM_{10}) mode. The TM_{10}-mode suggests that there is a variation in the field of the first $\lambda\ /2$ cycles straight the length of the patch, but there is no diversity straight the width with the patch. The MPA is depicted as two slots in the following Figure 2.17, which are segregated by the means of the transmission line of length L and have open circuits at both the beginning and the end of the line.

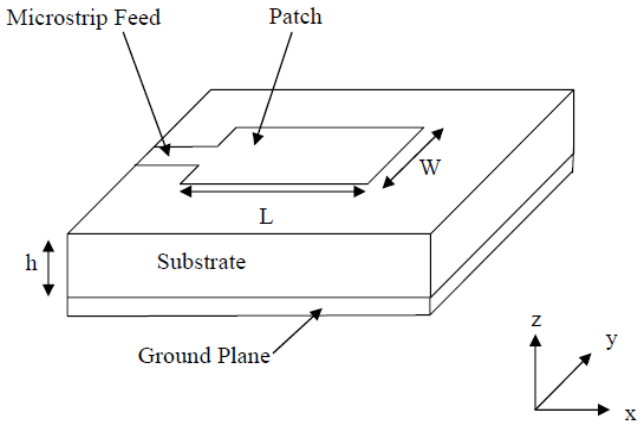

Figure 2.16: Arrangement of the MPA [37].

Because of the open ends, the current is at its lowest point straight with the width of the patch, where the voltage is at its highest level. When the fields at the edges are considered in relation to the ground plane, it is possible to dissect them into their normal and tangential components [36].

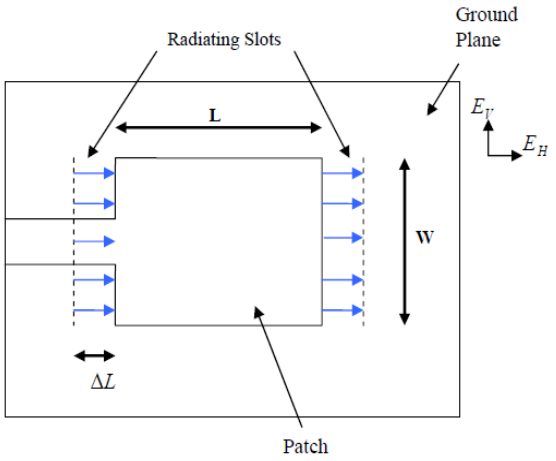

Figure 2.17: Top view of antenna [37].

Since the patch is $\lambda/2$ long, the ordinary components for the E-field at the couple of the edges straight with the width are in adverse directions, making them out of phase. Because of this, they eliminate the each other out in the broadside direction, as shown in Figure 2.18. The fact that the tangential components (which can be seen in Figure 2.18) are in phase indicates that the outcoming fields converge to provide the utmost radiated field in a direction that is a normal to the surface of the structure.

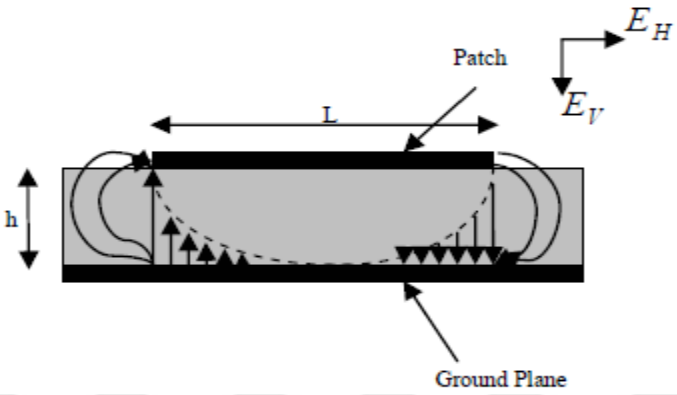

Figure 2.18: Side view of antenna [37].

There are a couple of the radiating slots in phase with each other, and they radiate into the half-space above the ground plane as a result of their positions along the width. These slots are 0.5λ apart from one another and are excited simultaneously. It is possible to model the fringing fields straight with the width as radiating slots, and electrically the patch of the MPA is emerges to be larger than its actual size. Because of the fringing effect, which is represented by the equation in [36], [37] the dimensions of the patch have been extended on both ends through a distance equal to ΔL along its length.

$$\Delta L = 0.412h\frac{\left(\varepsilon_{reff}+0.3\right)\left[\frac{W}{h}+0.264\right]}{\left(\varepsilon_{reff}-0.258\right)\left[\frac{W}{h}+0.8\right]} \tag{2.8}$$

In this instant, the effective length for the radiated patch of the MPA can be written as follows:

$$l_{effective} = L + 2\Delta L \tag{2.9}$$

In the case of the given value of the operating frequency, we can obtain the effective length of the radiated patch of the MPA as follows:

$$l_{effective} = \frac{c}{2f_o\sqrt{\varepsilon_{reff}}} \quad (2.10)$$

Where:

c: indicate to the light speed in the free space; and

f_o: indicate to the antenna operating frequency.

Finally, the MPA radiated patch width can be obtained by utilizing the following mathematical relation:

$$W = \frac{c}{2f_o\sqrt{0.5(\varepsilon_r + 1)}} \quad (2.11)$$

2.4.2 Cavity Model

The method of analysing that known as the transmission line models which was presented and discussed in the subsection that came before this one is easy to utilise, but it bears from a number of drawbacks that are discussed further on. Because it bypasses the field differences at the radiating borders, the utilization of it for the design of the rectangular MPA is efficient and effective. These challenges can be conquered by employing the cavity model in the appropriate situations. The information that follows is a condensed summary of this model. This modelling depicts the internal zone of the dielectric substrate as a cavity that is bordered on all sides by the electric walls located at the upper and the lower of the structure. The following points can be applied for thin dielectric substrates like ($h << \lambda$) support this method [37], [38]:

a) As a result of the thin substrate, the fields in the internal zone do not tumble significantly in the z-direction (in other words, in a manner that is typical of the patch).
b) The electric field is only z-directed at the area that is bordered by the patch metallisation and the ground plane of the MPA, whereas the magnetic field contains only the transverse components at that location (Hx and Hy). This assertion serves as the conceptual foundation for both the top and bottom electric walls.

Take a look at Figure 2.19 shown below, once the power is applied from the source to the MPA, the distributions of the charges appear on the patch's topmost and down surfaces, as well as at the ground plane's bottom. Two means govern the charge distribution: the first one is the attracting mechanism, and the latter is the repulsive. The ground plane and the opposing charges at the nethermost portion of the radiating patch form the attracting means that helps keep the condensation of the charges at the under most of the patch unchanged. The repulsive means occur within the similar charges on the patch's bottom exterior, causing certain charges to be pushed from the bottom to the top. Currents stream at the upper and the lower exteriors of the patch as a result of the charge motion [39].

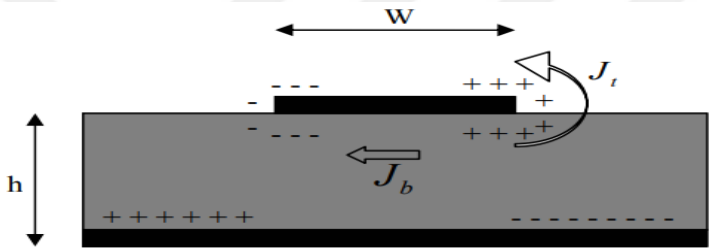

Figure 2.19: Distribution of charges on the MPA patch [39].

Because the elevation to width ratio (i.e., the thickness of the substrate to the W) is so minimal in the cavity model, the attractive means dominate, causing the majority of the charge condensation and current to lie beneath the patch exterior. An extremely smaller current would flow on the top exterior of the patch, and as the height to width ratio was further decreased, the current on the top surface of the patch would be nearly zero, preventing the generation of any tangential E-field components to the patch edges. This would happen because the height to width ratio was further decreased.

2.4.3 Full-Wave Analysis Model

The Method of Moments is one of the strategies that introduced to provide a complete wave analysing for the MPAs. Surface currents are utilized for the modelling of the MPA, while volume polarisation currents are employed to simulate the dielectric sheet fields in this approach. It has been demonstrated how to obtain integral equations for these unfamiliar currents, and how to turn these integral equations to the matrix equations employing the "Method of Moments", which may

then be solved using different algebraic approaches to yield the results. Usually, some of the software can be utilised to do the analysis such as the Ansys HFSS [40].

2.5 FREQUENCY SELECTIVE SURFACES (FSS)

Meta surfaces are a type of planar metamaterial that has a thickness that is subwavelength, and they are referred to as "MSs" Lithography and nano-printing are two processes that can be used to produce Meta surfaces easily. Both of the metamaterials and MSs are developing swiftly as research areas, and their application enables the spatial modification of electromagnetic or optical responses, in addition to scattering phase, amplitude, and polarization. By making use of the appropriate materials and design, the ultra-thin construction of MSs has the potential to significantly reduce destructive and unwanted losses along the direction in which waves propagate. When it comes to polarization response, every MS is categorized according to the working regulation or capabilities of the array element (FSS, high impedance surfaces, ideal absorbers, reflecting surfaces, and so on). One of the structures that make up an MS is called an FSS, and all it does is demonstrate an electric comeback. Only the electrical polarization may have been adequate up until this point for tailoring the frequency selectiveness in both the transmission and the reflection features. Based on the theory of antennas and the engineering of microwaves, such surfaces are frequently fabricated by utilizing a planar and periodical matrix of metallic patches or strips with distinguishable figures. This construction method is derived from the theory of antennas and microwave engineering. In order to modify the EM waves that strike them and to construct the dispersive transmitted or reflected characteristic, the FSS is utilized. The FSSs are typically created by placing periodic arrays of metallic segments on a dielectric substrate. This is the most common method. It's possible that the amplitude of the transmitted wave will change when it's in phase with the wave that's coming in from the opposite direction. In any event, the selection can be applied to the polarization of the incident light in order to accentuate abnormalities in the emission pattern. These abnormalities can take the form of a change in the phase or amplitude of the wave that is transmitted. The type of modification that is made to the transmitted wave can determine the degree to which a variety of implementations that are related to the various conditions can be simplified. According to the physical structure, the scope, and the geometry of the filter, there are four different types of FSS filters. These filters are high pass, low pass, bandpass, and bandstop filters. The concept of the Babinet has been instrumental in the

transformation of band-stop FSSs into band-pass FSSs and vice-versa, as well as in the conversion of low-pass FSSs into high-pass FSSs. As can be seen in Figure 2.20, the high-pass FSS can be thought of as Babinet's equivalent to the low-pass FSS, and the similar is true for the band-pass and band stop FSS. In addition, the band-pass and band stop FSS are shown below. According the filtering capabilities of the FSS, it has the potential to operate as a series of parallel RLC circuits. Figure 2.20 illustrates the analogous circuits as well as the associated filter responses for a variety of filter types. The FSS patches will be responsible for producing the R and L, while the spaces in amidst the FSS patches will be responsible for producing the C. Electrostatic information, such as the capacitance of a parallel plate capacitor and the inductance of a pair of parallel wires, can be used to describe the physical meaning of these C and L values of various FSS. Other examples of electrostatic information included as in [41].

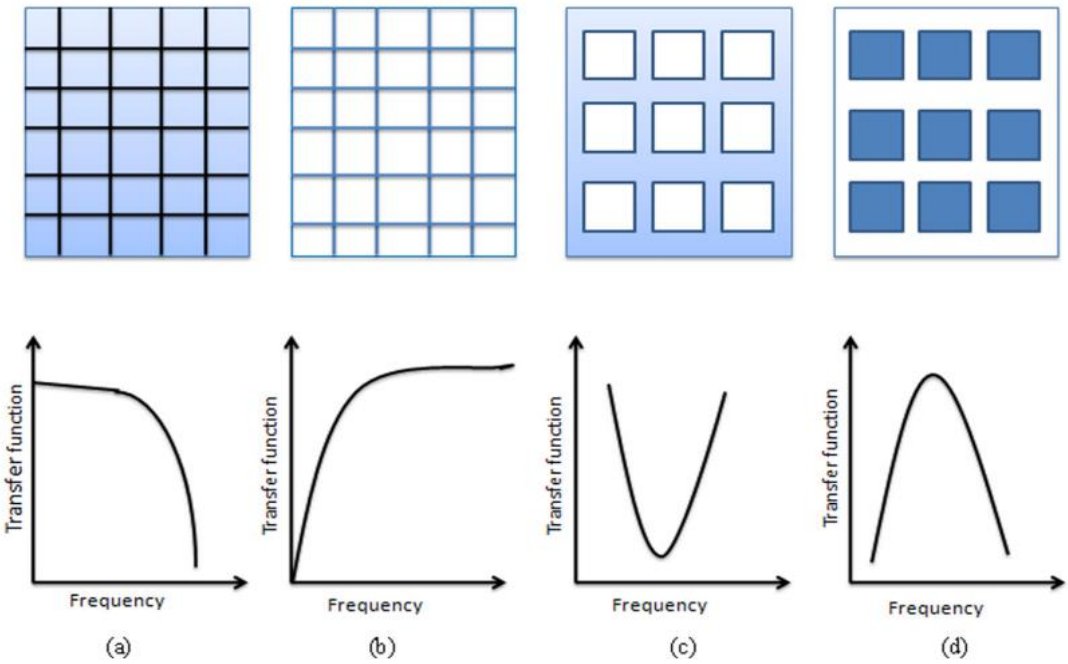

Figure 2.20: Characterization of the FSS with its own response, **(**a) solid patch structure act as a low-pass, (b) slot array structure act as a high-pass (c) loop elements act as band-stop, and (d) loop slot structure act as band-pass filter [41].

Figure 2.21 depicts the diagrammatic representations for the previously mentioned groups. A complementary self-resonating network, as shown in Figure 2.22, can be used to visualize the FSS implementation. In simple words, when an electromagnetic wave strikes the FSS structure, electric currents are induced.

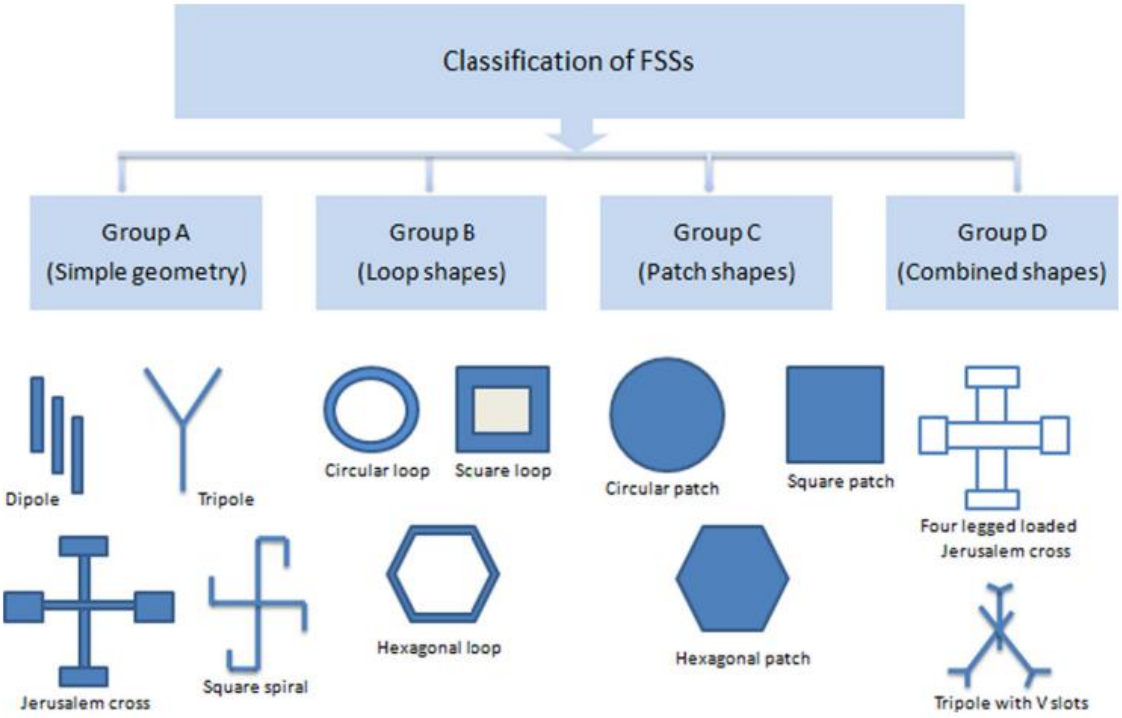

Figure 2.21: Collection for the basic possible structures for the FSSs [41].

The induced currents' amplitude is determined by the coupling of the energy level. These generated a current that act as electromagnetic origins, resulting in more distributed fields. As a result, the general field in the area of FSS is made up of incident electromagnetic fields and scattered fields. The collection (A) consists of dipole class patches segments that are organized to operate as bandstop filters for incident plane waves as well as entire reflecting surfaces across a restricted frequency range, as illustrated in Figure 2.21. The slot class aperture segments, like those in group B, have passband qualities, meaning they proceed as semi-reflecting surfaces to incident electromagnetic waves at the working frequency range. Nonetheless, the structures shown in Figure 2.21 have inadequate filter response, low angular stability, and unreasonable BW, making them only appropriate for the narrow range of the electromagnetic implementations [41].

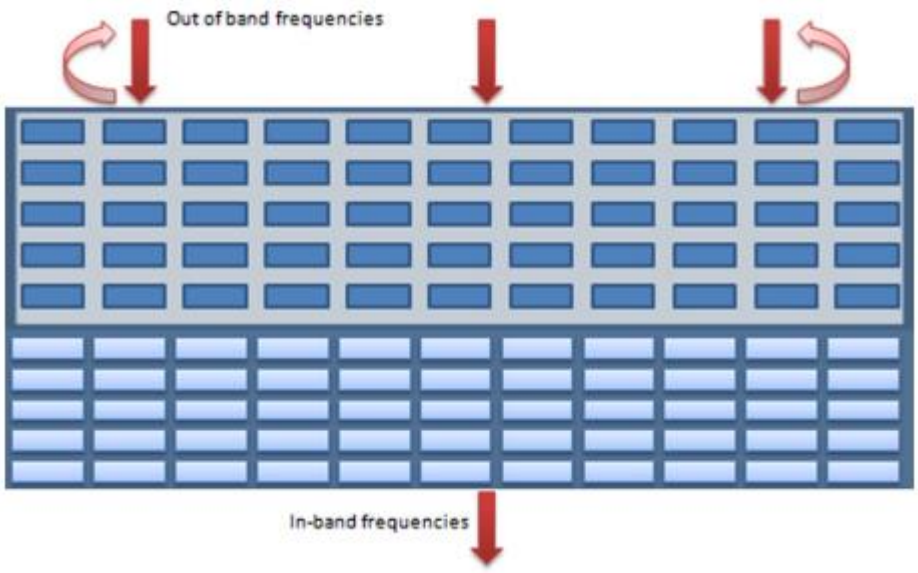

Figure 2.22: The applicable definition for FSS [41].

2.6 WORKING OF FSS

According to the principles of circuit theory, FSS structures (both capacitive and inductive) can be thought of as analogous to microwave filters. As was mentioned earlier, the FSS filtering features can be broken down into four primary categories, and each of these categories fulfills a particular function. Low pass FSS filters allow a more limited frequency range to pass through the configuration, while simultaneously allowing a wider frequency range to pass unimpeded. In accordance with the Babinet principle, the operation of a high-pass FSS filter is analogous to the opposite of that of a low-pass FSS filter. In a similar vein, an FSS filter with a stopband eliminates frequencies that are not wanted, whereas an FSS filter with a passband restricts the frequency range that is allowed to pass. For the purpose of providing the desired resonant function, FSSs are constructed using periodic arrays of metal patches and/or slots that have been engraved on a dielectric substrate. The selection of the appropriate FSS array elements, shapes, dimensions, and substrate materials is the step in the design procedure that bears the heaviest burden of responsibility [42].

3. ANTENNA DESIGN AND ANALYSING

3.1 INTRODUCTION

In this chapter of the thesis, we will explain the basic stages of designing this work, which is to design antennas and improve their parameters. In addition, in this chapter the achieved results from this work will be clearly illustrated and discussed.

3.2 METHODOLOGY

In this work, a small-sized rectangular and circular shape of the MPA is introduced to have functioned in the indoor environment of the government institutions for the private networks over the frequency band of 62 GHz. The utilization of this band will help employees to transfer large size of data at a very high data transfer speed within the internal network, which will contribute to reducing waiting time, latency, and smoothing work. In order to optimize the antenna performance, the FSS superstrate from the square and circular shape is utilized to be situated above the MPA with a specifically prescribed air gap, as shown in Figure 3.11.

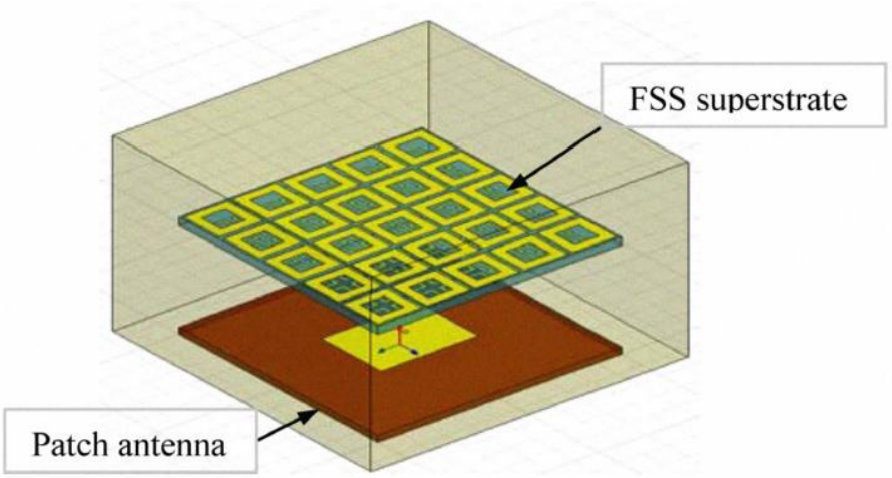

Figure 3.1: Configuration for the proposed work.

In addition, an investigation for the introduced MPA and FSS will be evaluated on the following manner:

a) Conventional rectangular MPA with a square shape FSS
b) Conventional rectangular MPA with a circular shape FSS

3.3 CONVENTIONAL RECTANGULAR MPA DESIGN

In order to design the conventional MPA, the designer needs to keep in mind a number of fundamental and significant points throughout the design process, which can be summed up as follows:

a) MPA operation frequency (f_r): This is the frequency over which the antenna will operated. In this work the f_r is selected to be 62 GHz.
b) The dielectric material constant (ε_r): This is the relative permittivity of the substrate which specified by the manufacturing company. In the work the utilized substrate is Rogers RT5880 which have an $\varepsilon_r = 2.2$.
c) The thickness of the dielectric material (i.e., substrate): This is the height of the substrate which is selected in this work to be $h = 0.1mm$.

After selecting After finishing the process of the specifying the elemental parameters that were mentioned above, the process of calculating the antenna dimensions begins. For this purpose, the simple analysis method of the transmission line that has been discussed in section (2.4.1) and for the method equations evaluation the MATLAB software is used. Once the dimensions are acquired the simulation process is initiates by build the 3D structure for the conventional MPA inside the CST simulation software framework. The dimensions description for the conventional MPA coupled with the feeding are shown in Figures 3.2.

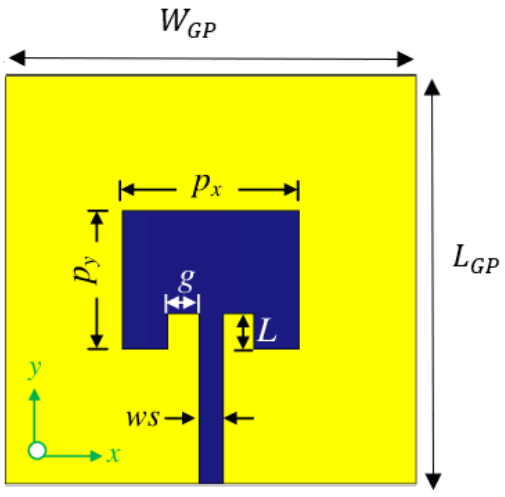

Figure 3.2: Dimensions illustration for the conventional MPA.

The simulated conventional rectangular MPA is shown in Figure 3.3 and the calculated dimensions for the rectangular shape conventional MPA are presented in Table 3.1.

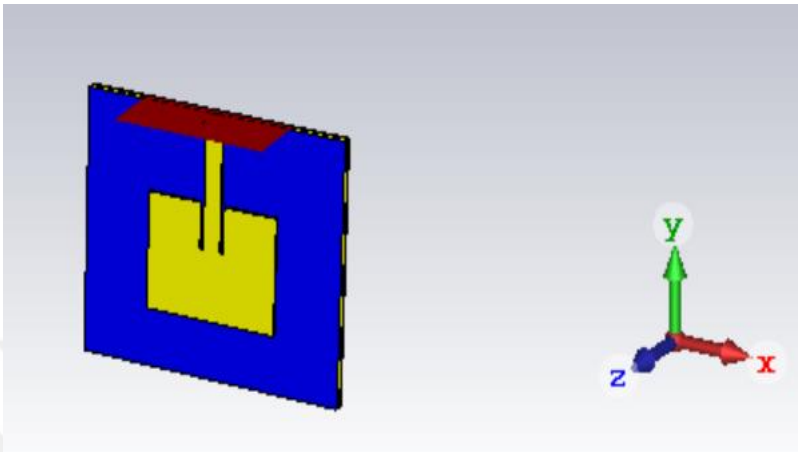

Figure 3.3: Conventional rectangular MPA within the simulation software.

Table 3.1: Calculated Conventional MPA dimensions.

Dimension	**Size in (mm)**
Length of the Patch (P_y)	1.767
Width of the Patch (P_x)	1.911
Length of the Ground Plane (L_{GP})	3.534
Width of the Ground Plane (W_{GP})	3.822
Length of the Strip Line (L_S)	1.767
Width of the Feed Line (W_S)	0.308
Feeding Insert in the Patch (L)	0.537
Separation Between Strip Line and Patch (G)	0.037

When calculating the antenna dimensions, it is noticed that there is a shift in the resonant frequency from the desired frequency (meaning 62 GHz), so this problem must be solved. One of the more traditional methods is the process of the modification of the antenna dimensions, in which the

special dimensions of the patch and transmission line are reduced or increased. Table 3.2 shows the final antenna dimensions after the modification process.

Table 3.2: Modified conventional MPA dimensions.

Dimensions	P_y	P_x	L_{GP}	W_{GP}	L_S	W_S	L	G
Modified Size (mm)	1.535	1.97	3.07	3.94	1.76	0.26	0.6	0.05

3.4 SQUARE FSS DESIGN

In this work, the FSS superstrate is placed above of the conventional MPA, segregated like a cavity via a specific an air gap, is realized to enhancing the parameters of the conventional antenna and make the antenna more intelligent to passes only the required frequencies. In this paper, the square FSS shape is chosen due to it is characterized by the best performance of the other available shapes. The proposed FSS design is made from copper with a thickness of 0.035 mm and printed over an Arlon AD300 dielectric material with a thickness of 0.1 mm and an $\in_r$ of 2.65. The introduced single-cell FSS design in this work is illustrated in Figure 3.4 and the single cell dimensions are illustrated in Table 3.3.

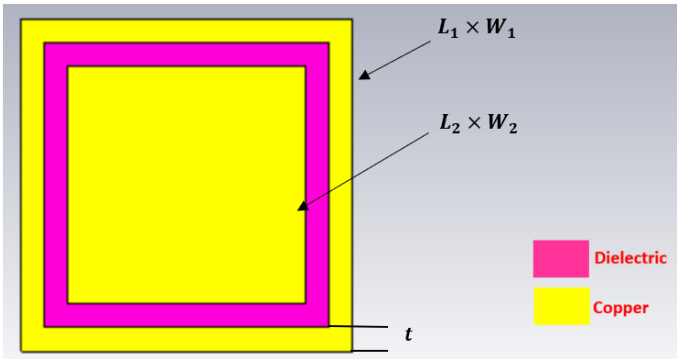

Figure 3.4: Single square FSS cell.

Once the single cell design is completed the construction of the FSS matrix is done by copying the single cell as an element in the matrix configuration. The proposed matrix comprised of a 4×4 elements, as shown in Figure 3.5.

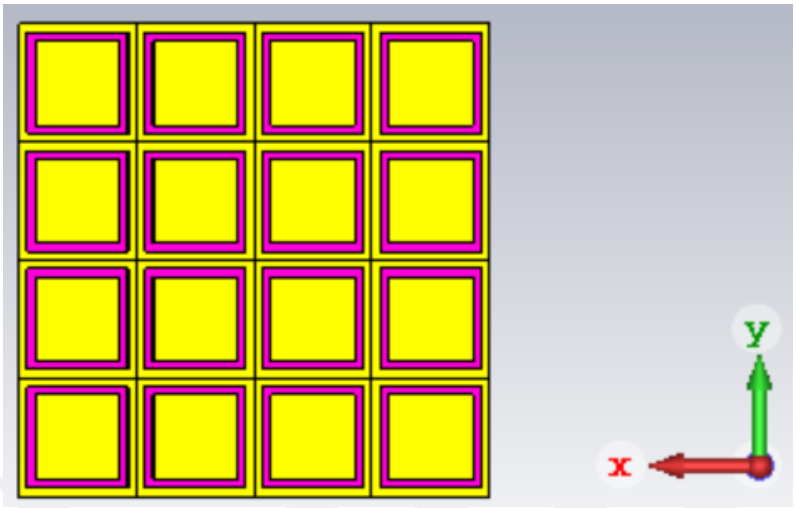

Figure 3.5: Square FSS matrix.

The proposed antenna configuration is consisting of a conventional rectangular MPA and 4×4 FSS substrate matrix sited over which with a distance of 2.1 mm, as illustrated in Figure 3.6.

Table 3.3: Dimensions for the single cell of FSS.

Dimension	Size (mm)
Outer Frame Length (L_1)	1.40
Outer Frame Width (W_1)	1.4
Square Patch Length (L_2)	1.0
Square Patch Width (W_2)	1.0
Outer Frame-Patch Spacing	0.10
Outer Frame Thickness (t)	0.20
Substrate Thickness	0.1
Copper Thickness	0.07

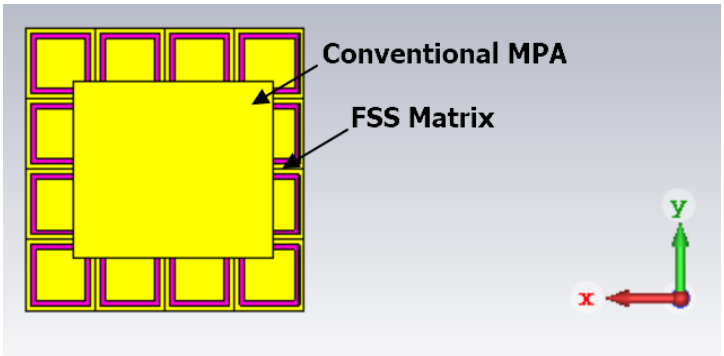

(a) Back view

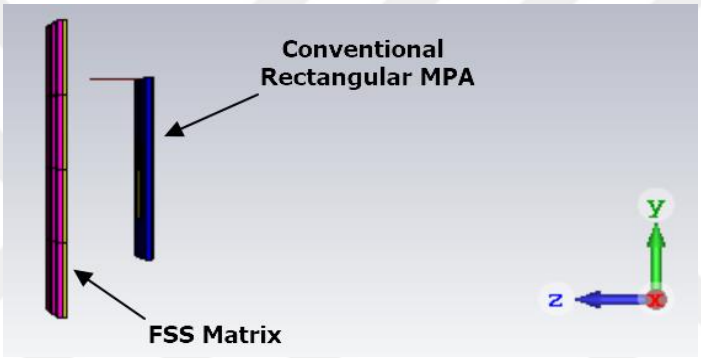

(b) Side View

Figure 3.6: Proposed antenna configuration.

In order to examine the performance of the square FSS matrix, a unit cell is simulated inside the CST. Since the $S_{11} < -10$ dB and S_{21} around the 0 dB the FSS is able to pass the required frequency, as shown in Figure 3.7.

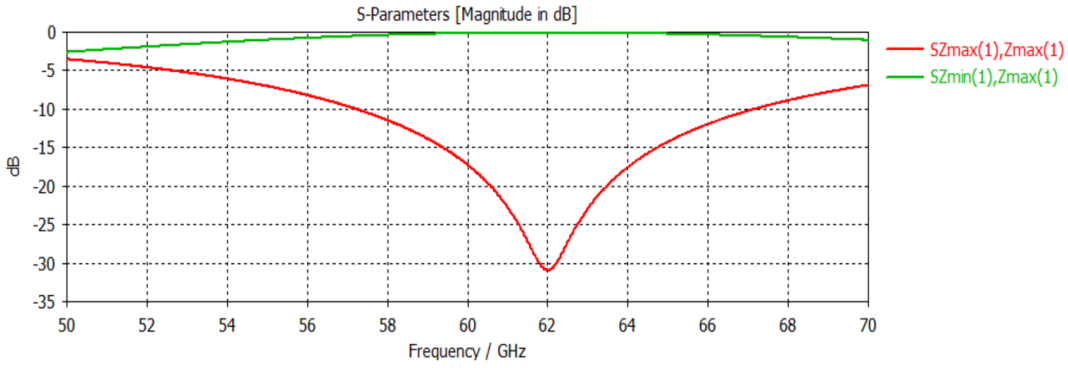

Figure 3.7: S-parameters for the square FSS single cell.

3.5 CIRCULAR FSS DESIGN

In this section the procedure for the design of the single cell for the FSS from the circular shape. The proposed design is comprising of a square dielectric substrate from the same material that has been utilized in the design of the square FSS (i.e., Arlon AD300) with a thickness of 0.1 mm. The squared substrate is covered by a square copper layer with a thickness of 0.035 mm. Over the square copper layer, a circular patch is engraved in the centre with a diameter of 1.1 mm and isolated from the rest of the copper flake by an air gap with of 0.021 mm. The simulated circular FSS single cell is illustrated in Figure 3.8 and its dimensions is illustrated in Table 3.4.

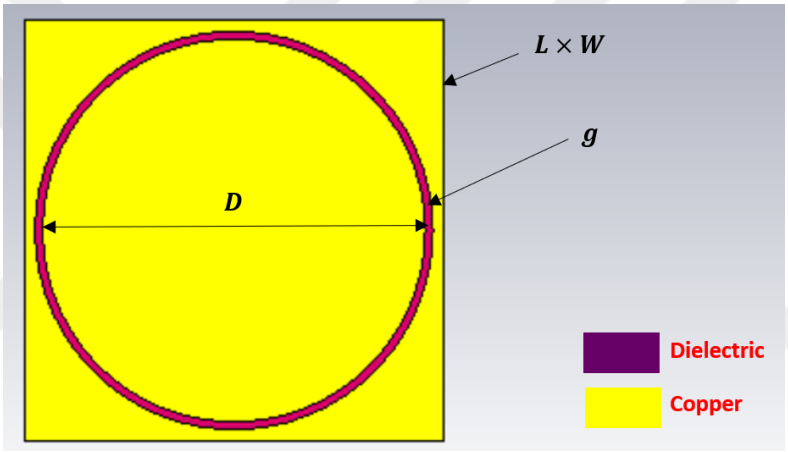

Figure 3.8: Single circular FSS cell.

Table 3.4: Dimensions for the single cell of FSS.

Dimension	Size (mm)
Base Length (L)	1.20
Base Length (W)	1.20
Circular Patch Diameter (L_2)	1.090
Outer Frame-Patch Spacing (g)	0.020
Substrate Thickness	0.10
Copper Thickness	0.070

Once the single cell design is completed, the next step summarized by simulate it within the CST environment. After that, the construction of the FSS matrix is done by copying the single cell as

an element in the matrix configuration. The simulate circular FSS matrix comprised of a 4×4 elements, as shown in Figure 3.9.

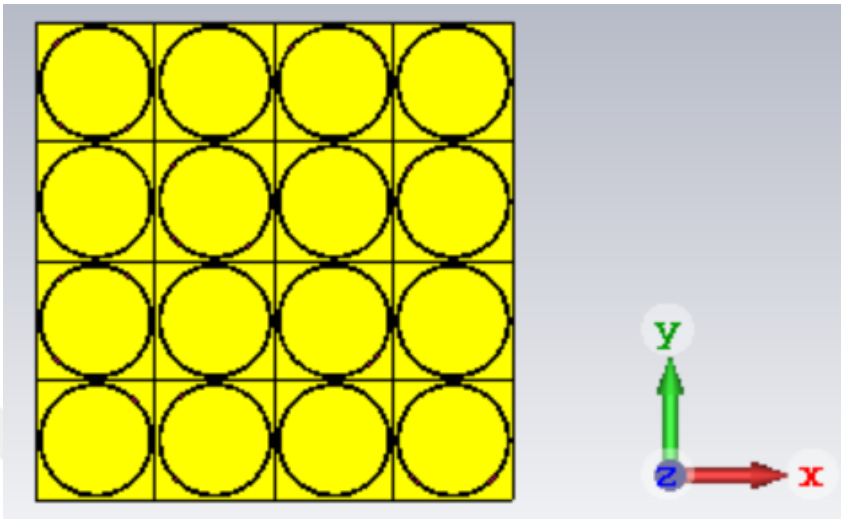

Figure 3.9: Circular FSS matrix.

After completion the simulation procedure for the circular FSS matrix, we will study its effects on the conventional rectangular MPA. The proposed antenna now is consisting of a conventional rectangular MPA and 4×4 circular FSS substrate matrix sited over which with a distance of 2.1 mm. Figure 3.10 illustrates the side view and the back view for the conventional rectangular MPA with the circular shape FSS matrix.

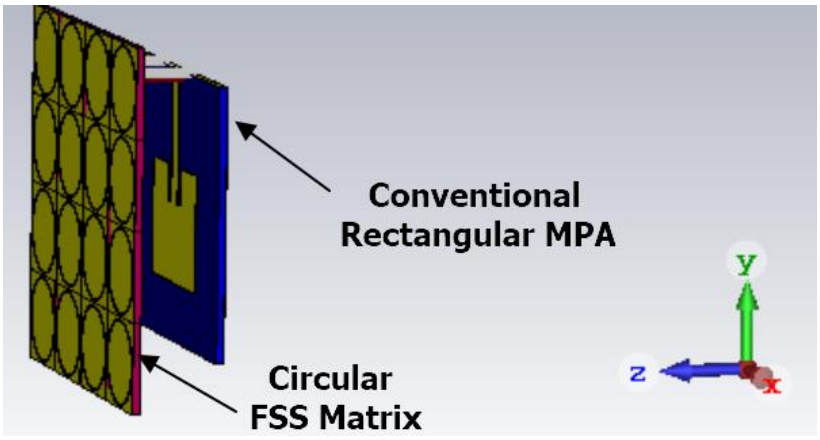

Figure 3.10: Conventional circular MPA with circular FSS matrix.

In order to examine the performance of the circular FSS matrix, a unit cell is simulated inside the CST. Since the $S_{11} < -10$ dB and S_{21} around the 0 dB the FSS is able to pass the required frequency, as shown in Figure 3.11.

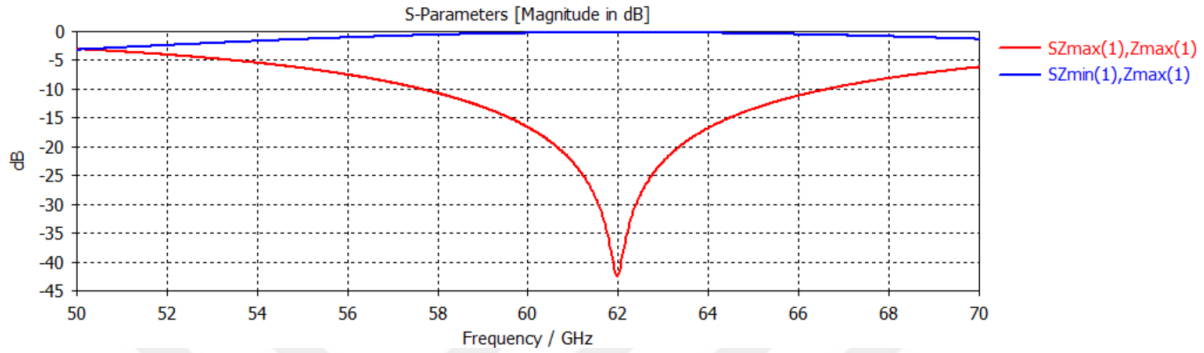

Figure 3.11: S-parameters for the circular FSS single cell.

3.6 SIMULATION RESULTS

In the section of this thesis chapter, we will clearly illustrate and discussed the obtained results from the antenna simulation software for the different designed antennas (i.e., conventional rectangular MPA with and without the FSS matrices).

3.6.1 Return Loss

The Return Losses (RL) of the antenna can be summarized and interpreted as the portion of the electrical power supplied to the antenna, which is reflected or returned to the source supplied the power due to the impedance mismatch between the source and the antenna feed line. The antenna manufacturers and the scientists suggested that the antenna works properly when these losses are less than or equal to -10 dB, which means that the antenna has received most of the electrical power supplied by the means of the source, which is 90% of the supplied power, and the remaining 10% is reflected in the direction of the source due to the mismatch in impedance.

A) RL for the conventional rectangular MPA

The acquired RL results for the conventional rectangular MPA before the process of the parameter modification is presented in Figure 3.12.

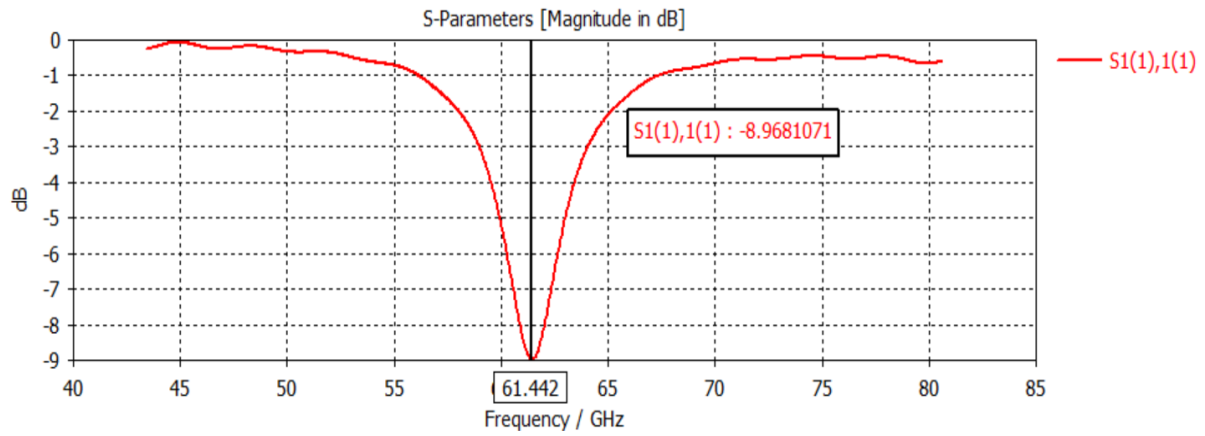

Figure 3.12: RL for the conventional rectangular MPA before the parameter modification.

As seen in the previous Figure 3.10 the RL of the antenna equals -8.96 dB which signifies that there is a big mismatching in the impedance, as well the $f_r = 61.442\ GHz$ which is inconsistent with the desired frequency (i.e., $f_r = 62\ GHz$). In order to overcome this problem, we should apply the parameter modification process which means increasing or decreasing the dimensions of the antennas. This process can be done via the utilizing of the different algorithms or by the traditional way of the trial and error. In this work the trial-and-error procedure have applied due to the simplicity and the low execution time. Figure 3.13 shows the RL for the conventional rectangular MPA after the parameter modifications.

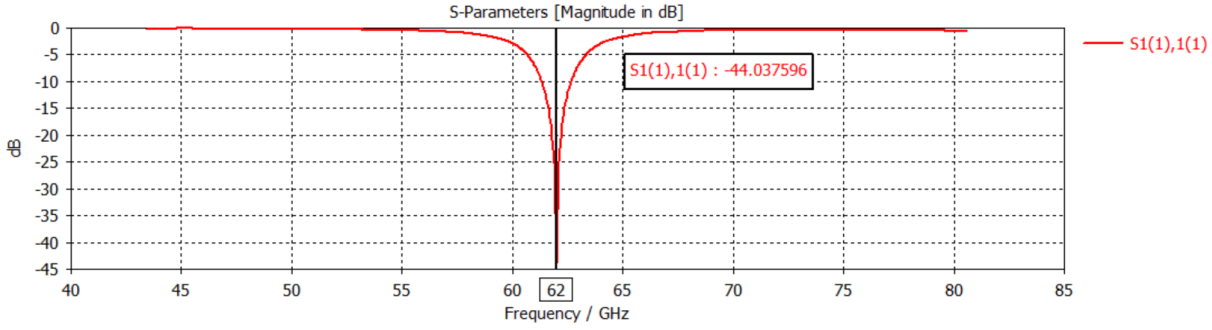

Figure 3.13: RL for the conventional rectangular MPA after the parameter modifications.

It is clear that from the previous Figure 3.13, the RL for the antenna is enhanced to be equals -44.03 dB and the frequency of operation is shifted to the required (i.e., $f_r = 62\ GHz$). This due to the positive impact of the parameter modification process that has been applied for the purpose of

the solving the impedance mismatching problem that affecting the overall performance of the simulated antenna.

B) RL for the conventional rectangular MPA with square FSS matrix

The acquired RL results for the conventional rectangular MPA with the square FSS matrix is presented in Figure 3.14.

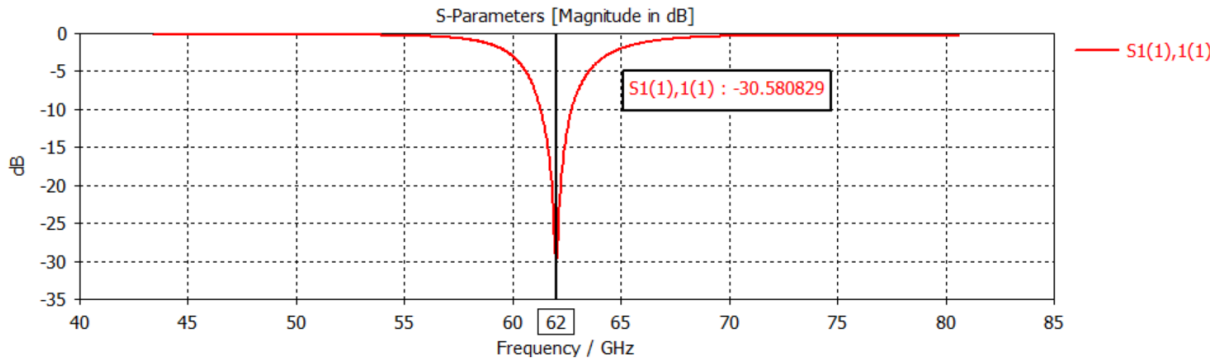

Figure 3.14: RL for the conventional rectangular MPA with square FSS matrix.

As seen from the previous Figure 3.14, the RL of the antenna with the square matrix FSS equals -30.58 dB. As compared with that of modified parameters conventional rectangular MPA, the RL of the previous case is better but the antenna is still functioning properly and efficiently since the RL is less than -10 dB.

C) RL for the conventional rectangular MPA with circular FSS matrix

The acquired RL results for the conventional rectangular MPA with the circular FSS matrix is presented in Figure 3.15.

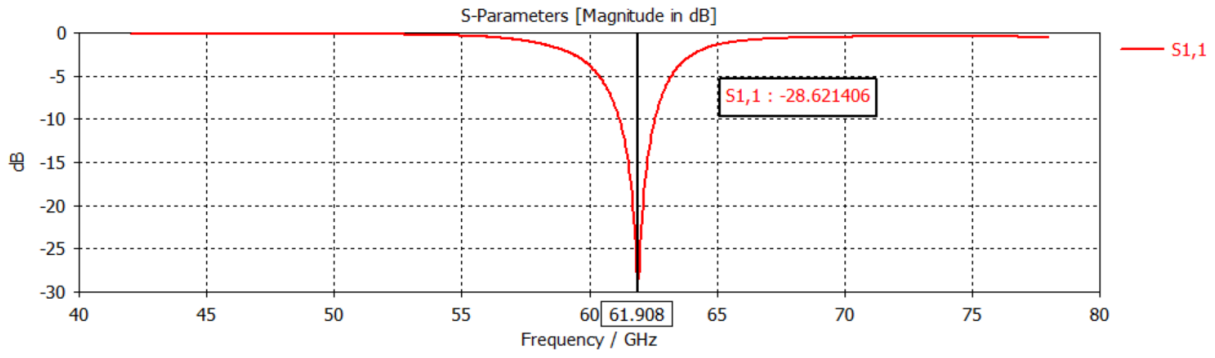

Figure 3.15: RL for the conventional rectangular MPA with circular FSS matrix.

As presented from the previous Figure 3.15, the RL of the antenna with the square matrix FSS equals -28.62 dB. As compared with that of modified parameters conventional rectangular MPA and the conventional rectangular MPA with the square FSS matrix, the RL of the previous cases is better but the antenna is still functioning properly and efficiently because the RL is remains within the good acceptable range (i.e., $RL < -10$ dB).

3.6.2 Bandwidth

Briefly, the Bandwidth (BW) of the antenna can be interpreted as the package or set of the frequencies on the left and right side of the antenna f_r in which the antenna parameters approximately have the same values as that calculated at the f_r. The BW is usually obtained from the RL pattern at the $RL = -10\ dB$ by utilising the measurement illustration lines that offered by the simulation software.

A) BW for the conventional rectangular MPA

The BW for the modified parameters conventional rectangular MPA is equals 1.323 GHz, as shown in Figure 3.16.

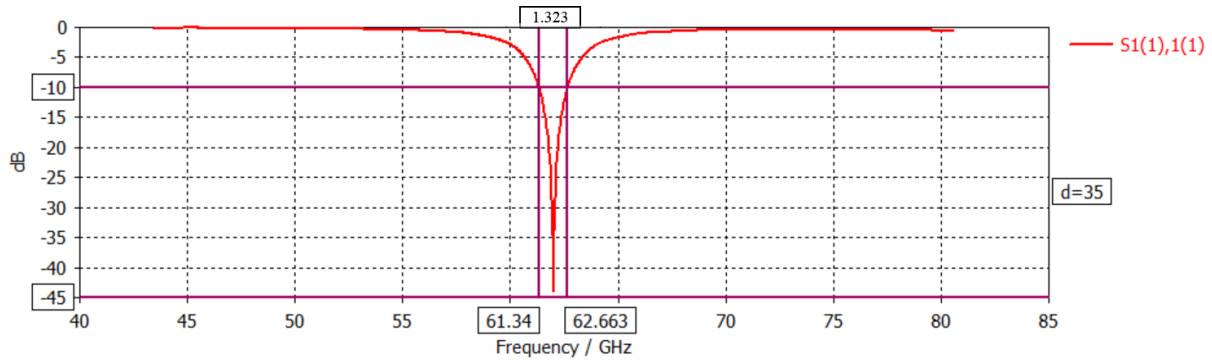

Figure 3.16: BW for the conventional rectangular MPA after the parameter modification.

B) BW for the conventional rectangular MPA with square FSS matrix

The acquired BW results for the conventional rectangular MPA with the square FSS matrix is equals 1.57 GHz, as presented in Figure 3.17.

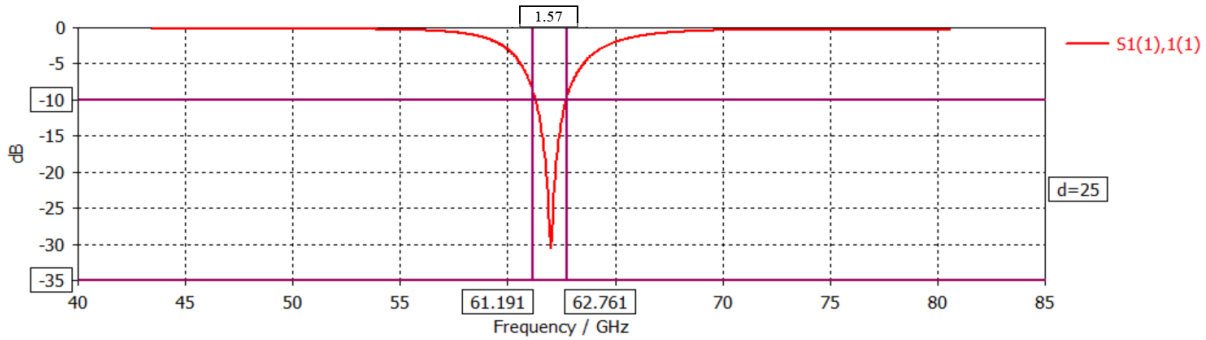

Figure 3.17: BW for the conventional rectangular MPA with the square FSS matrix.

C) BW for the conventional rectangular MPA with circular FSS matrix

The acquired BW results for the conventional rectangular MPA with the circular FSS matrix is equals 1.58 GHz, as presented in Figure 3.18.

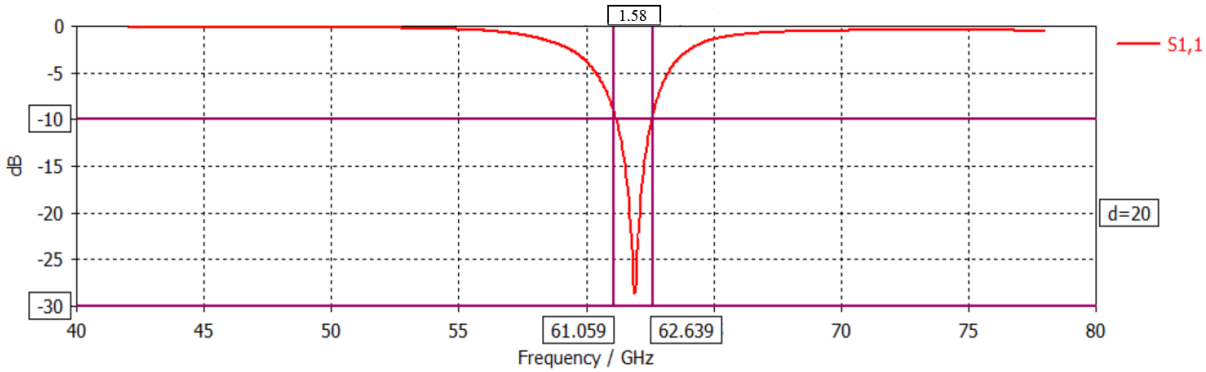

Figure 3.18: BW for the conventional rectangular MPA with the circular FSS matrix.

The BW of the antenna is determined through the subtracting of the lower frequency (f_L) from the upper frequency (f_H), in the simulation software this procedure is done automatically as presented in the previous figures. According to the acquired simulation results the BW for the conventional rectangular MPA has been boosted after installing the FSS matrices. In order to summarise the acquired BW results for the previous configurations Table 3.5 is introduced.

Table 3.5: Comparison results for the introduced antennas.

Antenna	f_L (GHz)	f_H (GHz)	BW (MHz)
Conventional MPA	61.34	62.663	1323
Conventional MPA with square FSS	61.191	62.761	1570
Conventional MPA with circular FSS	61.059	62.639	1580

3.6.3 Gain

One of the most significant parameters for the antennas is the antenna gain which shows the ability of the antenna to how converting the electric power into radiated power or vice versa. For the conventional MPA, the gain is related to two factors. The first one is the height of the MPA substrate, whereas there is a proportional relationship between the gain and the height. The second one is the constant of the substrate, whereas there is an inversely proportional between the dielectric constant of the substrate and the gain of the antenna.

A) Gain for the conventional rectangular MPA

Figure 3.19 presents the gain for the conventional rectangular MPA after the parameter modification process which is equals 7.21 dBi.

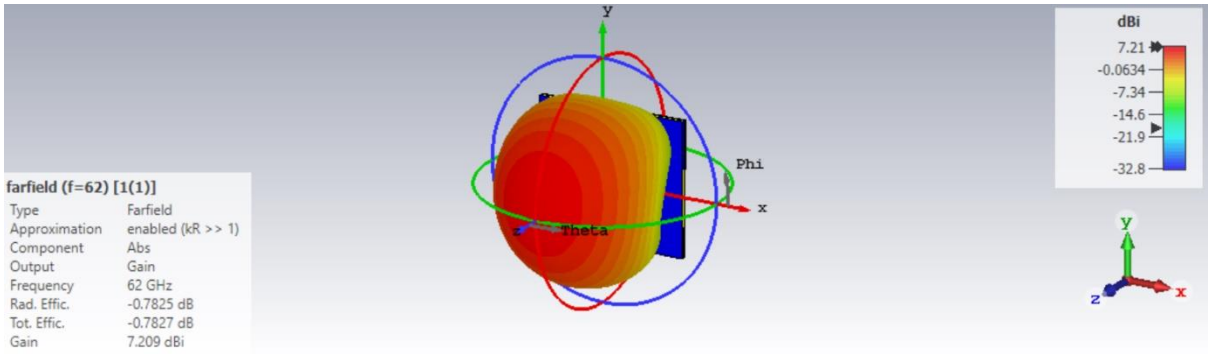

Figure 3.19: Gain for the conventional rectangular MPA.

According the obtained gain for the previous design, this value is reasonable but there is need to enhance this parameter by employing the FSS metrices.

B) Gain for the conventional rectangular MPA with square FSS matrix

Figure 3.20 presents the gain for the conventional rectangular MPA after adding the square FSS matrix which is equals 10.6 dBi.

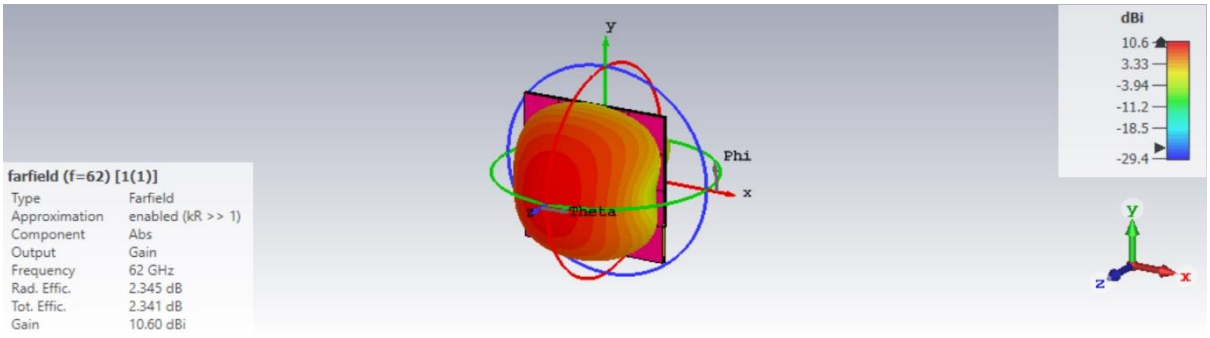

Figure 3.20: Gain for the conventional rectangular MPA with the square FSS matrix.

C) Gain for the conventional rectangular MPA with circular FSS matrix

Figure 3.21 presents the gain for the conventional rectangular MPA after adding the circular FSS matrix which is equals 10.9 dBi.

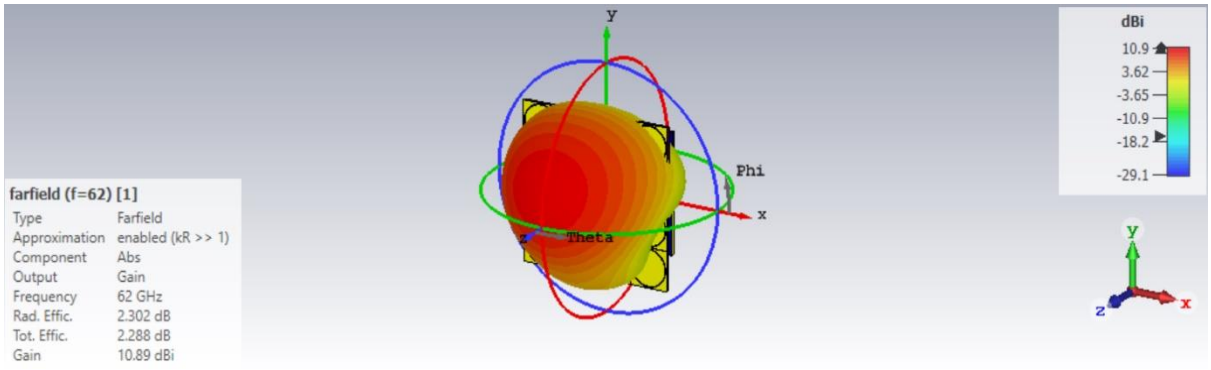

Figure 3.21: BW for the conventional rectangular MPA with the circular FSS matrix.

According to the acquired simulations results for the gain that are demonstrated in the three-dimensional form in the Figures 3.19-3.21, there is a significant enhancement after adding the FSS metrices. In the term of the best gain is achieved after adding the circular FSS matrix which is differs from the square FSS by just 0.3 dBi which considered a very slight enhancement. In the

term of the ease of the design, simulation, and manufacturing the square shape is better also it offers more stability in the analysis. In order to demonstrate the enhancement for the gain after adding the FSS metrices Table 3.6 is developed.

Table 3.6: Comparison results for the introduced antennas.

Design	Gain in (dBi)
Conventional MPA	7.21
Conventional MPA with square FSS	10.6
Conventional MPA with circular FSS	10.9

3.6.4 Radiation Pattern

The radiation pattern of the any antenna is interpreted as the shape of the power that is really emitted away from the antenna. The beamwidth of the antenna is the essential factor or parameter that can be controlled an antenna with a high or poor gain. Whereas there is an inversely proportional between the gain and the beamwidth once the beamwidth is narrow the gain increased because the power is concentrated into a small angle contributing to a higher gain. In the case of the wider beamwidth here the power is divides over the wide angles and lead to make the antenna gain is low. Often the beamwidth in the two planes appears to be identical but this is not general means.

A) Radiation pattern for the conventional rectangular MPA

Figure 3.22 presents the radiation pattern for the conventional rectangular MPA after the parameter modification. In this figure we can see that the beamwidth is equals 82.6° which is to some extent considered as a wide beam.

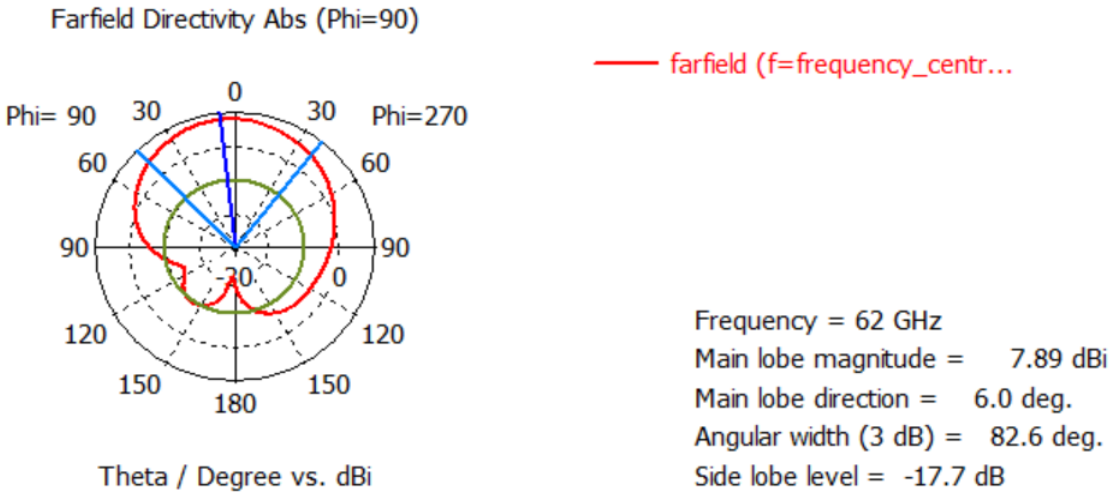

Figure 3.22: Radiation pattern for the conventional rectangular MPA.

B) Radiation pattern for the conventional rectangular MPA with square FSS matrix

Figure 3.23 presents the radiation pattern for the conventional rectangular MPA after adding the square FSS matrix. It clearly demonstrated from the figure the beamwidth is narrower than that without FSS matrix. In order to make the beamwidth narrower the stopband FSS matrix can be utilized and installed under the ground plane of the antenna or utilizing the antenna array configuration, where this can be controlled according to the required application.

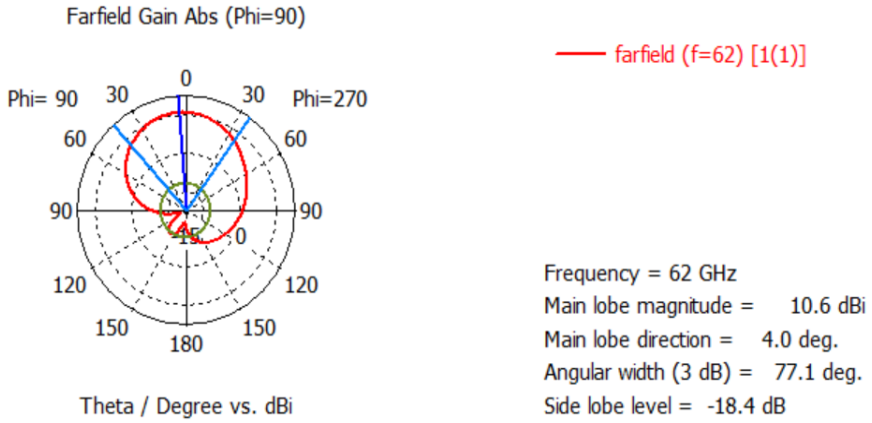

Figure 3.23: Radiation pattern for the conventional rectangular MPA with square FSS matrix.

C) Radiation pattern for the conventional rectangular MPA with square FSS matrix

Figure 3.24 presents the radiation pattern for the conventional rectangular MPA after adding the circular FSS matrix. It is clear from the next figure the beamwidth is narrower than the both previous cases.

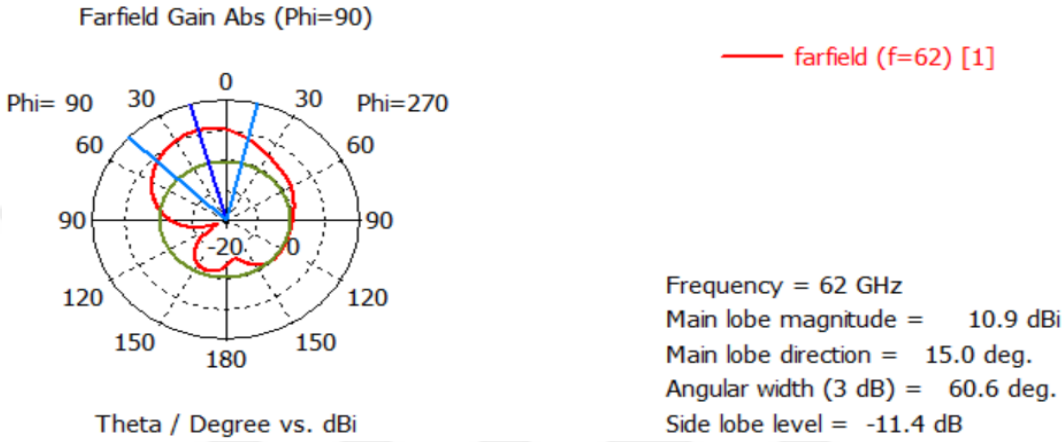

Figure 3.24: Radiation pattern for the conventional rectangular MPA with square FSS matrix.

In order to demonstrate the enhancement for the antenna parameters such as the antenna RL, BW, gain results, and the radiation pattern after parameter modifications, square FSS matrix, as well as circular FSS matrix we summarized the obtained results from the antenna simulation software in Table 3.7.

Table 3.7: Comparison results for the designed antennas.

Design	RL (dB)	BW (MHz)	Gain (dBi)	Radiation Pattern (degree)
Conventional Rectangular MPA	-44.03	1323	7.21	82.6°
Conventional Rectangular MPA with Square FSS	-30.58	1570	10.6	77.1°
Conventional Rectangular MPA with Circular FSS	-28.62	1580	10.9	60.6°

It is clear that from the previous Table 3.6 there isn't an ideal antenna, this signifies that each of the simulated designs makes the enhancement for the specific parameters and leaves the other parameters constant or with a slight degradation. In order to specify the enhancement for the parameters in each case Table 3.8 is introduced.

Table 3.8: Parameters enhancement for the designed antennas.

Design	**RL (dB)**	**BW (MHz)**	**Gain (dBi)**	**Radiation pattern (degree)**
Conventional Rectangular MPA	Best	Lowest	Lowest	Wider
Conventional Rectangular MPA with Square FSS	Acceptable	Enhanced	Enhanced	Enhanced
Conventional Rectangular MPA with Circular FSS	Acceptable	Better	Better	Better

4. CONCLUSION AND FUTURE WORK

4.1 CONCLUSION

In the past few years, wireless communications have developed dramatically, becoming an essential component of daily life. This led to a very huge increase in the number of applications connected with wireless networks, which contributed to the occurrence of crowding and a decrease in the speed of data transmission. In order to solve the aforementioned problem, it was suggested to use high frequencies, especially unlicensed ones, due to the large range and their ability to provide a very high data transfer speed. Most MPAs suffer from several problems, most of which are related to low gain and narrow bandwidth. In this work, a compact conventional rectangular MPA has been simulated and designed based on the CST antenna analysing software for the private networks inside the government institutions over the 62 GHz frequency band. In order to solve the conventional MPA related problems, the FSS passband superstate has been suggested to be utilized and installed over the conventional antenna. After adding the FSS superstrate the antenna gain and bandwidth have been particularly improved. In addition, another design for the FSS matrix has been utilized from the circular shape and a comparison of results was made. According to the simulation results, we conclude that the antenna parameters have been improved slightly than the square shape. But in the term of the simplicity in the design and analysis, the square shape is the better.

4.2 FUTURE WORK

The science of antennas is vast in terms of diversity in design and optimization approaches. In order to develop and improve the performance of this work, there are several modifications that can be added, which are summarized as follows:

a) Constructing a stopband FSS matrix and installing under the conventional rectangular MPA to enhance the parameters of the antenna.
b) Using the metamaterials and printed over the same substrate of the antenna to minimize the antenna size.
c) Using the antenna array arrangement to increase the antenna efficiency and obtained narrower beamwidth.

REFERENCES

[1] Shankar, P. M., "Introduction to wireless system", New York: Wiley, pp. 22-52, 2002.

[2] Osseiran, A., Monserrat, J. F., & Marsch, P., "5G mobile and wireless communications technology", Cambridge University Press, 2016.

[3] Kumar, S., "Wireless Communications Fundamental & Advanced Concepts: Design Planning and Applications", River Publishers, Vol. 41, 2015.

[4] Bandyopadhyay, L. K., Chaulya, S. K., & Mishra, P. K., "Wireless communication in underground mines", RFID-Based Sens. Netw, Vol. 22, 2010.

[5] Yilmaz, T., Gokkoca, G., & Akan, O. B., "Millimetre wave communication for 5G IoT applications. In Internet of Things (IoT)", in 5G Mobile Technologies, Springer, Cham, pp. 37-53, 2016.

[6] Al-Falahy, Naser, and Omar YK Alani. "Millimetre wave frequency band as a candidate spectrum for 5G network architecture: A survey." Physical Communication, vol. 32, pp.120-144, 2019.

[7] Chittimoju, G., & Yalavarthi, U. D., "A Comprehensive Review on Millimeter Waves Applications and Antennas", In Journal of Physics: Conference Series, IOP Publishing, vol. 1804, no. 1, pp. 1-7, 2021.

[8] El Oualkadi, A., "Trends and challenges in CMOS design for emerging 60 GHz WPAN applications", InTech, 2011.

[9] Chataut, R., & Akl, R., "Massive MIMO systems for 5G and beyond networks—overview, recent trends, challenges, and future research direction", Sensors, vol.20, no.10, pp.1-22, 2020.

[10] Kliks, A., Holland, O., Basaure, A., & Matinmikko, M., "Spectrum and license flexibility for 5G networks", IEEE Communications Magazine, vol.53, no.7, pp.42-49, 2015.

[11] Laya, A., Wang, K., Widaa, A. A., Alonso-Zarate, J., Markendahl, J., & Alonso, L., "Device-to-device communications and small cells: enabling spectrum reuse for dense networks", IEEE Wireless Communications, vol.21, no.4, pp. 98-105, 2014.

[12] Baltaci, A., Dinc, E., Ozger, M., Alabbasi, A., Cavdar, C., & Schupke, D., "A Survey of Wireless Networks for Future Aerial Communications (FACOM)", IEEE Communications Surveys & Tutorials, vol. 1, no. 3, pp. 1-3, 2020.

[13] Sur, S., Pefkianakis, I., Zhang, X., & Kim, K. H., "Wifi-assisted 60 GHz wireless networks", In Proceedings of the 23rd Annual International Conference on Mobile Computing and Networking, pp. 28-41, 2017.

[14] Paul, L. C., Pramanik, R. K., ur Rashid, M. M., Hossain, M. N., Mahmud, M. Z., & Islam, M. T., "Wideband Inset Fed Slotted Patch Microstrip Antenna for ISM Band Applications", In 2019 Joint 8th International Conference on Informatics, Electronics & Vision (ICIEV), IEEE, pp. 79-84, 2019.

[15] Nissan, U. N., Singh, G., Kumar, P., & Kumar, N., "High Gain Terahertz Microstrip Array Antenna for Future Generation Cellular Communication", In 2020 International Conference on Artificial Intelligence, Big Data, Computing and Data Communication Systems (icABCD), IEEE, pp.1-6, 2020.

[16] Yang, W., Ma, K., Yeo, K. S., & Lim, W. M., "A compact high-performance patch antenna array for 60-GHz applications", IEEE Antennas and Wireless Propagation Letters, vo.15, pp. 313-316, 2015.

[17] Outerelo, D. A., Alejos, A. V., Sanchez, M. G., & Isasa, M. V., "Microstrip antenna for 5G broadband communications: Overview of design issues", In 2015 IEEE International Symposium on Antennas and Propagation & USNC/URSI National Radio Science Meeting, IEEE, pp. 2443-2444, 2015.

[18] Mohsen, M. K., Jowad, R. R., & Mousa, A. H., "Performance of microstrip patch antenna for single and array element with and without EBG", Periodicals of Engineering and Natural Sciences (PEN), vol.9, no.3, pp.22-28, 2021.

[19] Amin, S., Ahmed, B., Amin, M., Abbasi, M. I., Elahi, A., & Aftab, U., "Establishment of boundaries for near-field, fresnel and Fraunhofer-field regions", In 2017 IEEE Asia Pacific Microwave Conference (APMC), IEEE, pp. 57-60, 2017.

[20] Milligan, T. A., "Modern antenna design", John Wiley & Sons, 2005.

[21] Rusch, W. V. T., & Potter, P. D., "Analysis of reflector antennas", Academic Press, 2013.

[22] Mailloux, R. J., "Phased array antenna handbook", Artech house, 2017.

[23] Rashid, S. Z., Gafur, A., Ullah, A., Hossain, M., Mamun, S. S., Majumder, M., & Alahi, Q. E., "Maximum Power Design and Simulation for a Low Return Loss Wearable Microstrip Patch Antenna", In Towards a Wireless Connected World: Achievements and New Technologies, Springer, Cham, pp. 161-175, 2022.

[24] Elfergani, I., Hussaini, A. S., Rodriguez, J., & Abd-Alhameed, R. (Eds.), "Antenna fundamentals for legacy mobile applications and beyond", New York, NY, USA: Springer International Publishing, pp. 1-659, 2019.

[25] Rana, S., Thakur, A., Saini, H. S., Kumar, R., & Kumar, N., "A wideband planar inverted F antenna for wireless communication devices", In 2016 International Conference on Advances in Computing, Communication, & Automation (ICACCA)(Spring), IEEE, pp. 1-3, 2016.

[26] Chowdhury, S. G., Arefin, M. S., & Faisal, M. M. A., "Design Simulation and Analysis of a Dual-Band Microstrip Patch Antenna for GPS and WLAN Applications", 2021.

[27] Wang, T., Chen, G., Zhu, J., Gong, H., Zhang, L., & Wu, H., "Deep understanding of impedance matching and quarter wavelength theory in electromagnetic wave absorption", Journal of Colloid and Interface Science, vol.595, pp.1-5, 2021.

[28] Nahar, T., & Rawat, S., "Efficiency enhancement techniques of microwave and millimeter-wave antennas for 5G communication: A survey", Transactions on Emerging Telecommunications Technologies, vol. e4530, 2022.

[29] Mishra, R., "An overview of microstrip antenna", HCTL Open International Journal of Technology Innovations and Research (IJTIR), vol. 21, no. 2), pp. 39-55, 2016.

[30] Prabowo, A. S., Pambudiyatno, N., & Harianto, B. B., "Microstrip Antenna Design with Patch Rectanguler for Primary Surveillance Radar (PSR) L-Band Application", In Journal of Physics: Conference Series, IOP Publishing, vol. 1845, no. 1, p. 012033, 2021.

[31] Singh, I., & Tripathi, V. S., "Micro strip patch antenna and its applications: a survey", Int. J. Comp. Tech. Appl, vol. 2, no. 5, pp. 1595-1599, 2019.

[32] Pathak, S., & Singh, S. K., "Microstrip Patch Antenna: A Review and the Current State of the Art", International Research Journal of Engineering and Technology (IRJET), vol. 8, no. 6, 2395-0072, 2021.

[33] Prakasam, V., & Reddy, N., "Design and simulation of elliptical micro strip patch antenna with coaxial probe feeding for satellites applications using matlab", In 2020 Fourth International Conference on I-SMAC (IoT in Social, Mobile, Analytics and Cloud) (I-SMAC), IEEE, pp. 228-234, 2020.

[34] Mishra, R., "An overview of microstrip antenna", HCTL Open International Journal of Technology Innovations and Research (IJTIR), vol. 21, no. 2, pp. 39-55, 2016.

[35] Aboserwal, N., Ramos, N. R. C., Qamar, Z., & Salazar-Cerreno, J. L., "An accurate analytical model to calculate the impedance bandwidth of a proximity coupled microstrip patch antenna (PC-MSPA)", IEEE Access, vol. 8, pp. 41784-41793, 2020.

[36] Kaushik Vipul, R., & Panchal, J. R., "Dielectric resonator antenna and its design parameters-A review", Research Journal of Advanced Engineering and Science, vol. 2, vol. 4, pp. 128-133, 2017.

[37] Fang, D. G., "Antenna theory and microstrip antennas", CRC Press, 2017.

[38] Bernard, V., & Iloh, J. P. I., "Microstrip antenna design using transmission line model", International Journal of Emerging Technology and Advanced Engineering, vol.3, no.11, pp. 410-415, 2013.

[39] Fang, D. G., "Antenna theory and microstrip antennas", CRC Press, 2017.

[40] Balanis, C. A., "Antenna theory: analysis and design", John wiley & sons, 2015.

[41] Walia, S., Shah, C. M., Gutruf, P., Nili, H., Chowdhury, D. R., Withayachumnankul, W., & Sriram, S., "Flexible metasurfaces and metamaterials: A review of materials and fabrication processes at micro-and nano-scales", Applied Physics Reviews, vol. 2, no. 1, pp. 011303, 2015.

[42] Kapoor, A., Mishra, R., & Kumar, P. Frequen, "frequency selective surfaces as spatial filters: Fundamentals, analysis and applications.", Alexandria Engineering Journal, vol. 61, no. 6, pp. 4263-4293, 2022.